

Research Article

Universal Linear Precoding for NBI-Proof Widely-Linear Equalization in MC Systems

Donatella Darsena,¹ Giacinto Gelli,² and Francesco Verde²

¹Dipartimento per le Tecnologie, Università Parthenope, via Medina 40, I-80133 Napoli, Italy

²Dipartimento di Ingegneria Elettronica e delle Telecomunicazioni, Università Federico II, via Claudio 21, I-80125 Napoli, Italy

Received 1 May 2007; Accepted 1 September 2007

Recommended by Arne Svensson

In multicarrier (MC) systems, transmitter redundancy, which is introduced by means of finite-impulse response (FIR) linear precoders, allows for perfect or zero-forcing (ZF) equalization of FIR channels (in the absence of noise). Recently, it has been shown that the noncircular or improper nature of some symbol constellations offers an intrinsic source of redundancy, which can be exploited to design efficient FIR widely-linear (WL) receiving structures for MC systems operating in the presence of narrowband interference (NBI). With regard to both cyclic-prefixed and zero-padded transmission techniques, it is shown in this paper that, with appropriately designed precoders, it is possible to synthesize in both cases WL-ZF universal equalizers, which guarantee perfect symbol recovery for any FIR channel. Furthermore, it is theoretically shown that the intrinsic redundancy of the improper symbol sequence also enables WL-ZF equalization, based on the minimum meanoutput-energy criterion, with improved NBI suppression capabilities. Finally, results of numerical simulations are presented, which assess the merits of the proposed precoding designs and validate the theoretical analysis carried out.

Copyright © 2008 Donatella Darsena et al. This is an open access article distributed under the Creative Commons Attribution License, which permits unrestricted use, distribution, and reproduction in any medium, provided the original work is properly cited.

1. INTRODUCTION

Digital transmissions over frequency-selective channels are adversely affected by intersymbol interference (ISI). Such an impairment can be perfectly compensated for, or significantly reduced, by transmitting information-bearing data in a *block-based* fashion [1] and, at the same time, by using block finite-impulse response (FIR) equalizers at the receiver. Within the family of block-based communication technologies, the most commonly used schemes are the *discrete multi-tone* (DMT) one, which is employed in wireline applications, such as several digital subscriber line (xDSL) standards [2] and power line communications standards (HomePlug) [3], and the *orthogonal-frequency-division multiplexing* (OFDM) one, which is adopted in various wireless standards, such as IEEE 802.11a/g [4] and HIPERLAN2 [5], digital audio, and video broadcast (DAB/DVB) [6, 7].

Recently, a broad class of multicarrier (MC) block-oriented transmission schemes, including DMT and OFDM as special cases, has been introduced in [1, 8, 9] (see Section 2 for the system model). To counteract ISI by means of low-complexity block processing at the receiver, such MC schemes rely on *linear redundant precoding*, which enables

the following two-step equalization procedure: first, ISI between consecutive blocks, referred to as *interblock interference* (IBI), is eliminated and, then, ISI within symbols of a transmitted block, referred to as *intercarrier interference* (ICI), is removed. Two redundant precoding schemes [10] for IBI removal are widely considered in the literature. In the first one, a *cyclic prefix* (CP), of length L_r larger than or equal to the channel order L , is inserted at the beginning of each transmitted block; at the receiver, the CP is discarded and the remaining part of the MC symbol turns out to be IBI-free. The second scheme is based on *zero padding* (ZP), wherein $L_r \geq L$ zero symbols are appended to each symbol block; in this case, IBI suppression is obtained without discarding any portion of the received signal. If the number of zero symbols is equal to the CP length, CP- and ZP-based systems exhibit the same spectral efficiency.

As regards ICI mitigation, when the channel is quasistationary and channel-state information (CSI) is available at the transmitter, a sensible approach is to perform joint transmitter-receiver (transceiver) optimization [8, 9, 11]. However, in some wireless applications, CSI might be too costly to acquire; moreover, transceiver optimization be-

comes exceedingly complicated if the MC system operates in the presence of narrowband interference (NBI). Indeed, NBI is the major expected source of degradation both in wireless MC systems operating in overlay mode or in non-licensed band, and in wireline ones subject to crosstalk or radio-frequency interference. In these cases, a more viable solution consists of keeping the precoder fixed (e.g., by using an inverse discrete Fourier transform (IDFT)) and devising joint ICI and NBI suppression algorithms with manageable complexity at the receiver side.

Coming to performance limits, it is well-known (see, e.g., [8]) that, for CP-based systems, *linear* FIR (L-FIR) perfect or zero-forcing (ZF) ICI suppression (in the absence of noise) is *not* possible if the channel transfer function exhibits nulls on (or close to) some subcarriers, no matter how long the CP is. Even worse, removing the entire CP and imposing the ZF constraint consume all the available degrees of freedom in the synthesis of the L-FIR equalizer [12, 13], leading to the *unique* solution represented by the conventional receiver, which, in the given order, performs CP removal, discrete Fourier transform (DFT) and frequency-domain equalization (FEQ). In spite of its simple implementation, such a receiver lacks *any* NBI suppression capability [12–15]. On the other hand, ZP precoding enables *universal* FIR L-ZF equalization, that is, perfect symbol recovery is guaranteed *regardless* of the channel-zero locations [8, 9]. Compared with CP precoding, the price to pay for such an ICI suppression capability is the slightly increased receiver complexity and the larger power amplifier backoff. Additionally, since perfect IBI suppression is obtained by retaining the entire linear convolution of each transmitted block with the channel, the FIR L-ZF solution is not unique in the ZP case, even for a fixed equalizer order. This nonuniqueness allows one to gain some degrees of freedom for NBI suppression, which however might not be sufficient for synthesizing L-ZF equalizers with satisfactory performance in many NBI-contaminated scenarios (see Section 5).

Recently, with reference to a CP-based system employing IDFT precoding, it has been shown in [12] that, by exploiting the possible *improper* or *noncircular* [16, 17] nature of the transmitted symbols, improved NBI suppression capabilities can be attained by adopting *widely linear* (WL) FIR block-oriented receiving structures [18]. Specifically, a WL-ZF block equalizer has been devised in [12], which is able to gain the additional degrees of freedom needed to mitigate, in the minimum mean-output-energy (MMOE) [19] sense, the effects of the NBI at the receiver output. Exploitation of the noncircularity property has also been proposed in [12] for achieving blind channel identification. Along the same research line, the problem of perfectly equalizing FIR channels in block-based communication systems employing *linear nonredundant precoding* at the transmitter has been tackled in [20]. Many modulation formats of practical interest turn out to be improper [21–23], such as ASK, differential BPSK (DBPSK), offset QPSK (OQPSK), offset QAM (OQAM), MSK, and its variant Gaussian MSK (GMSK). In particular, the main advantage of staggered or offset modulation schemes, such as OQPSK and OQAM, with respect to their nonoffset counterparts, that is, QPSK and QAM, is the

increased bandwidth efficiency, which motivated their use in wireless [24, 25] and cable modem systems [26]. Moreover, offset modulation schemes are employed in pulse-shaping multicarrier systems [27] for their robustness to carrier frequency offset. It is worth noting that, in the MC context, noncircularity of the transmitted symbols has also been exploited to improve multiuser blind channel identification [28] and blind frequency-offset synchronization [29, 30].

Although the WL-ZF-MMOE equalizer proposed in [12] assures a significant performance advantage over the conventional L-ZF receiver in CP-based NBI-contaminated systems, it is not a universal one, since it is not able to perfectly suppress ICI when the channel transfer function has nulls on some subcarriers. Furthermore, the NBI suppression capabilities of the WL-ZF-MMOE equalizer have been tested only by computer simulations in [12]. Motivated by the importance of universal equalization, this paper builds on [12] and provides in Section 3 a detailed study of the conditions assuring WL-FIR perfect symbol recovery in both CP- and ZP-based systems. In particular, it is shown that, contrary to L-FIR equalization, universal WL perfect symbol recovery is possible not only in a ZP-based system, but also in a CP-based one, provided that the precoder satisfies some channel-independent design rules. Additionally, by gaining advantage of the results provided in Section 3, we generalize in Section 4 our previous formulation [12] of the WL-ZF-MMOE equalizer to both CP- and ZP-based systems and, in a general framework, we analyze its NBI rejection capabilities from a theoretical viewpoint. Finally, in Section 5, all the theoretical results provided throughout the paper are validated via numerical simulations, whereas concluding remarks are pointed out in Section 6.

1.1. Notations

Matrices (vectors) are denoted with upper case (lower case) boldface letters (e.g., \mathbf{A} or \mathbf{a}); the field of $m \times n$ complex (real) matrices is denoted as $\mathbb{C}^{m \times n}$ ($\mathbb{R}^{m \times n}$), with \mathbb{C}^m (\mathbb{R}^m) used as a shorthand for $\mathbb{C}^{m \times 1}$ ($\mathbb{R}^{m \times 1}$); $\{\mathbf{A}\}_{i_1 i_2}$ indicates the $(i_1 + 1, i_2 + 1)$ th element of matrix $\mathbf{A} \in \mathbb{C}^{m \times n}$, with $i_1 \in \{0, 1, \dots, m - 1\}$ and $i_2 \in \{0, 1, \dots, n - 1\}$; a tall matrix \mathbf{A} is a matrix with more rows than columns; the superscripts $*$, T , H , -1 , $-$, and \dagger denote the conjugate, the transpose, the Hermitian (conjugate transpose), the inverse, the generalized (1)-inverse [31], and the Moore-Penrose generalized inverse (pseudoinverse) [31] of a matrix; $\mathbf{0}_m \in \mathbb{R}^m$ denotes the null vector, $\mathbf{O}_{m \times n} \in \mathbb{R}^{m \times n}$ the null matrix, and $\mathbf{I}_m \in \mathbb{R}^{m \times m}$ the identity matrix; $\text{trace}(\cdot)$ represents the trace of a matrix for any $\mathbf{a} \in \mathbb{C}^n$, $\|\mathbf{a}\|$ denotes the Euclidean norm for any $\mathbf{A} \in \mathbb{C}^{n \times m}$, $\text{rank}(\mathbf{A})$, $\mathcal{N}(\mathbf{A})$, and $\mathcal{R}(\mathbf{A})$ denote the rank of \mathbf{A} , the null and the column space of \mathbf{A} ; $\mathbf{A} = \text{diag}[\mathbf{A}_{11}, \mathbf{A}_{22}, \dots, \mathbf{A}_{pp}] \in \mathbb{C}^{(np) \times (mp)}$, with $\mathbf{A}_{ii} \in \mathbb{C}^{n \times m}$, is a block diagonal matrix; finally, $E[\cdot]$ and \star denote ensemble averaging and convolution.

2. THE MC TRANSCIVER MODEL WITH LINEAR PRECODING AND WL EQUALIZATION

In this paper, we employ the generalized block-based transmit model developed in [8, 9], which encompasses many MC

communication systems, such as OFDM and DMT. At the receiver side, under the assumption that the transmitted symbols are improper, we resort to the WL block-by-block equalizing structure proposed in [12].

2.1. The MC signal model

Let us consider a multicarrier system with M subcarriers (see Figure 1), wherein the data stream $\{s(n)\}_{n \in \mathbb{Z}}$ is converted into M parallel substreams $s_m(n) \triangleq s(nM + m)$ for $m \in \{0, 1, \dots, M-1\}$. Any block of M consecutive symbols $\mathbf{s}(n) \triangleq [s_0(n), s_1(n), \dots, s_{M-1}(n)]^T \in \mathbb{C}^M$ is subject to a *linear redundant transformation* $\tilde{\mathbf{u}}(n) = \tilde{\mathbf{F}}\mathbf{s}(n)$, where $\tilde{\mathbf{u}}(n) \triangleq [\tilde{u}_0(n), \tilde{u}_1(n), \dots, \tilde{u}_{P-1}(n)]^T \in \mathbb{C}^P$, with $P \triangleq M + L_r > M$, and $\tilde{\mathbf{F}} \in \mathbb{C}^{P \times M}$ is a *full-column rank* (time-domain) precoding matrix to be designed. The redundancy $0 < L_r \ll M$ introduced for each transmitted block is the key to avoiding IBI at the receiver. Vector $\tilde{\mathbf{u}}(n)$ undergoes parallel-to-serial (P/S) conversion, and the resulting sequence feeds a digital-to-analog converter (DAC), operating at rate $1/T_c = P/T$, where T_c and T denote the sampling and symbol period, respectively. After up-conversion, the transmitted signal propagates through a physical channel modeled as a linear time-invariant filter, whose (composite) impulse response is $h_c(t)$ (encompassing the cascade of the DAC interpolation filter, the physical channel, and the analog-to-digital converter (ADC) antialiasing filter).

Let us assume, without loss of generality, that the n th symbol block $\mathbf{s}(n)$ has to be detected. To this aim, the received signal $\tilde{r}_c(t)$ is sampled, with rate $1/T_c$, at time instants $t_{n,\ell} \triangleq nT + \ell T_c$, with $\ell \in \{0, 1, \dots, P-1\}$, thus yielding the discrete-time sequence $\tilde{r}_\ell(n)$ for $\ell \in \{0, 1, \dots, P-1\}$. In the sequel, we set $h(m) \triangleq h_c(mT_c)$ and $\tilde{v}_\ell(n) \triangleq \tilde{v}_c(t_{n,\ell})$, where $\tilde{v}_c(t)$ represents the additive disturbance (NBI-plus-noise) at the receiver input, and we assume that the channel impulse response $h_c(t)$ spans $L \leq L_r$ sampling periods, that is, $h_c(t) = 0$ for $t \notin [0, LT_c]$; hence, the resulting discrete time channel $h(m)$ is a causal FIR filter of order $L \leq L_r$, that is, $h(m) = 0$ for $m \notin \{0, 1, \dots, L\}$, with $h(0), h(L) \neq 0$. By gathering the samples of the sequence $\{\tilde{r}_\ell(n)\}_{\ell=0}^{P-1}$ into the column vector $\tilde{\mathbf{r}}(n) \triangleq [\tilde{r}_0(n), \tilde{r}_1(n), \dots, \tilde{r}_{P-1}(n)]^T \in \mathbb{C}^P$, we obtain the following vector model [1, 8, 9] for the received signal:

$$\tilde{\mathbf{r}}(n) = \tilde{\mathbf{H}}_0 \tilde{\mathbf{F}}\mathbf{s}(n) + \tilde{\mathbf{H}}_1 \tilde{\mathbf{F}}\mathbf{s}(n-1) + \tilde{\mathbf{v}}(n), \quad (1)$$

where $\tilde{\mathbf{v}}(n) \triangleq [\tilde{v}_0(n), \tilde{v}_1(n), \dots, \tilde{v}_{P-1}(n)]^T \in \mathbb{C}^P$ is the disturbance vector, while $\tilde{\mathbf{H}}_0 \in \mathbb{C}^{P \times P}$ is a Toeplitz lower-triangular matrix [32] with first column $[h(0), h(1), \dots, h(L), 0, \dots, 0]^T$ and $\tilde{\mathbf{H}}_1 \in \mathbb{C}^{P \times P}$ is a Toeplitz upper-triangular matrix [32] with first row $(0, \dots, 0, h(L), h(L-1), \dots, h(1))$. In the rest of the paper, the following additional assumptions are considered:

(A1) the transmitted symbols $\{s(n)\}_{n \in \mathbb{Z}}$ are modeled as a sequence of zero-mean independent and identically dis-

tributed (i.i.d.) random variables, with variance $\sigma_s^2 \triangleq \mathbb{E}[|s(n)|^2] > 0$ and exhibiting the following property:

$$s^*(n) = e^{j2\pi\beta n} s(n) \quad \text{for } \beta \in [0, 1), \forall n \in \mathbb{Z}; \quad (2)$$

(A2) the disturbance $\tilde{v}_c(t) = \tilde{v}_{c,\text{nbi}}(t) + \tilde{v}_{c,\text{noise}}(t)$ is a zero-mean complex *proper* [33] wide-sense stationary (WSS) random process, statistically independent of the sequence $\{s(n)\}_{n \in \mathbb{Z}}$.

A sequence $s(n)$ satisfying assumption (A1) is *improper* [16], since $\mathbb{E}[s^2(n)] = \sigma_s^2 e^{-j2\pi\beta n} \neq 0$. Signals exhibiting property (2) are referred to in the literature as *conjugate symmetric* [34] and are encountered in telecommunications, radar, and sonar. They include all memoryless real modulation formats (BPSK, m -ASK), differential schemes (DBPSK), offset schemes (OQSPK, OQAM), and even (in an approximate sense) modulations with memory (binary CPM, MSK, GMSK). For example, real modulation schemes fulfill (2) with $\beta = 0$, that is, $s^*(n) = s(n)$, whereas for complex modulation schemes, such as OQPSK, OQAM, and MSK, relation (2) is satisfied [22, 23] if $\beta = 1/2$, that is, $s^*(n) = (-1)^n s(n)$. Remarkably, offset modulation schemes are employed in pulse-shaping multicarrier systems [27, 29, 30] for their robustness to carrier frequency offset. On the contrary, proper modulation schemes, such as m -QPSK, m -QAM, or m -PSK (with $m > 2$), exhibit $\mathbb{E}[s^2(n)] \equiv 0$ and, thus, they do not belong to the family of modulations satisfying assumption (A1).

2.2. IBI-free WL block processing

It has been shown in [12] that the linear dependence (2) existing between $s(n)$ and $s^*(n)$ might be regarded as an “intrinsic” redundancy contained in the original symbol sequence $s(n)$, which can be suitably exploited for synthesizing FIR-ZF equalizers with NBI suppression capabilities. This aim can be obtained by resorting to WL [18] processing of $\tilde{\mathbf{r}}(n)$, that is,¹

$$\mathbf{y}(n) = \tilde{\mathbf{G}}_1 \tilde{\mathbf{r}}(n) + \tilde{\mathbf{G}}_2 \tilde{\mathbf{r}}^*(n), \quad (3)$$

where $\tilde{\mathbf{G}}_1, \tilde{\mathbf{G}}_2 \in \mathbb{C}^{M \times P}$ are filtering matrices to be synthesized in order to jointly mitigate IBI, ICI, and disturbance. It is worthwhile to observe that, for the considered improper modulations, one obtains from (2) that $\mathbf{s}^*(n) = e^{j2\pi\beta n M} \mathbf{J}\mathbf{s}(n)$, where $\mathbf{J} \triangleq \text{diag}[1, e^{j2\pi\beta}, \dots, e^{j2\pi\beta(M-1)}] \in \mathbb{C}^{M \times M}$ is a *unitary* diagonal matrix. When $s(n)$ is real-valued ($\beta = 0$), it results that $e^{j2\pi\beta n M} \equiv 1$; whereas, when $s(n)$ is complex-valued ($\beta = 1/2$), it follows that $e^{j2\pi\beta n M} = (-1)^{nM}$. In the latter case, without loss of generality, we assume² that M is even, thus implying $(-1)^{nM} \equiv 1$.

¹ A FIR block equalizer can jointly elaborate multiple consecutive received blocks; herein, we focus our attention on the case where the equalizer elaborates only a single block $\tilde{\mathbf{r}}(n)$ (*zeroth-order block equalizer*).

² If M is odd, a preliminary “derotation” [12, 22, 23] of $\tilde{\mathbf{r}}^*(n)$ must be performed before evaluating $\mathbf{y}(n)$ in (3).

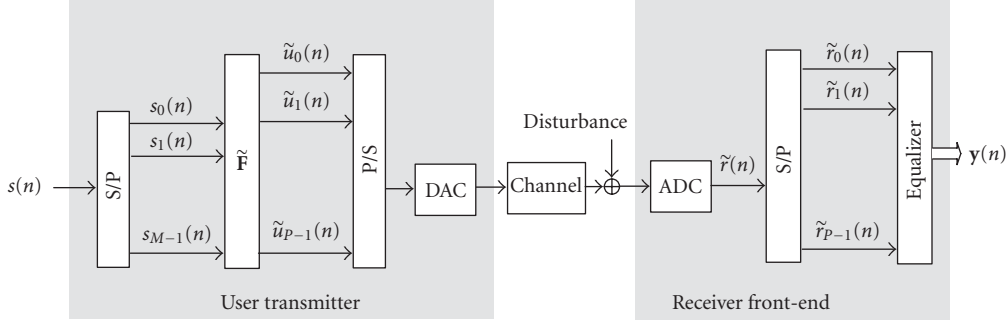


FIGURE 1: MC transceiver.

Accounting for (1), the equalizer output (3) assumes the form

$$\begin{aligned} \mathbf{y}(n) = & [\tilde{\mathbf{G}}_1 \tilde{\mathbf{H}}_0 \tilde{\mathbf{F}} + \tilde{\mathbf{G}}_2 \tilde{\mathbf{H}}_0^* \tilde{\mathbf{F}}^* \mathbf{J}] \mathbf{s}(n) \\ & + [\tilde{\mathbf{G}}_1 \tilde{\mathbf{H}}_1 \tilde{\mathbf{F}} + \tilde{\mathbf{G}}_2 \tilde{\mathbf{H}}_1^* \tilde{\mathbf{F}}^* \mathbf{J}] \mathbf{s}(n-1) \\ & + \tilde{\mathbf{G}}_1 \tilde{\mathbf{v}}(n) + \tilde{\mathbf{G}}_2 \tilde{\mathbf{v}}^*(n). \end{aligned} \quad (4)$$

To eliminate the IBI from the previous block [second summand in (4)], it can be observed that $\tilde{\mathbf{H}}_1$ has nonzero elements only in its $L \times L$ upper-rightmost submatrix. Relying on this fact, to perfectly nullify the IBI for any channel impulse response, it is sufficient to impose a structure on $\tilde{\mathbf{F}}$, $\tilde{\mathbf{G}}_1$, and $\tilde{\mathbf{G}}_2$ so that $\tilde{\mathbf{G}}_1 \tilde{\mathbf{H}}_1 \tilde{\mathbf{F}} = \tilde{\mathbf{G}}_2 \tilde{\mathbf{H}}_1^* \tilde{\mathbf{F}}^* = \mathbf{O}_{M \times M}$. For the sake of simplicity, we will adopt the choice $L_r = L$, which allows one to introduce the minimum redundancy at the transmitter. In this case, the desired structure can be forced by resorting to the following factorizations: $\tilde{\mathbf{F}} = \mathbf{T}\mathbf{F}$, $\tilde{\mathbf{G}}_1 = \mathbf{G}_1\mathbf{R}$, and $\tilde{\mathbf{G}}_2 = \mathbf{G}_2\mathbf{R}$, where $\mathbf{F} \in \mathbb{C}^{M \times M}$, $\mathbf{G}_1 \in \mathbb{C}^{M \times Q}$, and $\mathbf{G}_2 \in \mathbb{C}^{M \times Q}$ are free matrices, with \mathbf{F} being nonsingular, whereas $Q \geq M$, $\mathbf{T} \in \mathbb{R}^{P \times M}$, and $\mathbf{R} \in \mathbb{R}^{Q \times P}$ must be chosen such that $\mathbf{R}\tilde{\mathbf{H}}_1\mathbf{T} = \mathbf{R}\tilde{\mathbf{H}}_1^*\mathbf{T} = \mathbf{O}_{Q \times M}$. To this end, two different strategies [1, 8, 9] are commonly pursued:

- *ZP case*: $\mathbf{T} = \mathbf{T}_{zp} \triangleq [\mathbf{I}_M, \mathbf{O}_{M \times L}]^T \in \mathbb{R}^{P \times M}$, $\mathbf{R} = \mathbf{R}_{zp} \triangleq \mathbf{I}_P$, with $Q = P$;
- *CP case*: $\mathbf{T} = \mathbf{T}_{cp} \triangleq [\mathbf{I}_{cp}^T, \mathbf{I}_M]^T \in \mathbb{R}^{P \times M}$, $\mathbf{R} = \mathbf{R}_{cp} \triangleq [\mathbf{O}_{M \times L}, \mathbf{I}_M] \in \mathbb{R}^{M \times P}$, with $Q = M$ and $\mathbf{I}_{cp} \in \mathbb{R}^{L \times M}$ obtained from \mathbf{I}_M by picking its last L rows.

From a unified perspective, the equalizer output (4) can be rewritten in either cases as

$$\begin{aligned} \mathbf{y}(n) = & \underbrace{[\mathbf{G}_1, \mathbf{G}_2]}_{\mathbf{g} \in \mathbb{C}^{M \times 2Q}} \underbrace{\begin{bmatrix} \mathbf{H}\mathbf{F} \\ \mathbf{H}^*\mathbf{F}^*\mathbf{J} \end{bmatrix}}_{\mathcal{H} \in \mathbb{C}^{2Q \times M}} \mathbf{s}(n) \\ & + \underbrace{[\mathbf{G}_1, \mathbf{G}_2]}_{\mathbf{g} \in \mathbb{C}^{M \times 2Q}} \underbrace{\begin{bmatrix} \mathbf{R}\tilde{\mathbf{v}}(n) \\ \mathbf{R}\tilde{\mathbf{v}}^*(n) \end{bmatrix}}_{\mathbf{d}(n) \in \mathbb{C}^{2Q}} \end{aligned} \quad (5)$$

$$= \mathbf{g}\mathcal{H}\mathbf{s}(n) + \mathbf{g}\mathbf{d}(n),$$

where we have defined the channel matrix $\mathbf{H} \triangleq \mathbf{R}\tilde{\mathbf{H}}_0\mathbf{T} \in \mathbb{C}^{Q \times M}$. For the ZP case, it results that $\mathbf{H} = \mathbf{H}_{zp} \in \mathbb{C}^{P \times M}$ is a Toeplitz [32] matrix having $[h(0), h(1), \dots, h(L), 0, \dots, 0]^T$ as

first column and $[h(0), 0, \dots, 0]$ as first row. For the CP case, it results that $\mathbf{H} = \mathbf{H}_{cp} \in \mathbb{C}^{M \times M}$ is a circulant [32] matrix having $[h(0), h(1), \dots, h(L), 0, \dots, 0]^T$ as first column.

The matrices \mathbf{F} , \mathbf{G}_1 , and \mathbf{G}_2 must be designed in order to mitigate ICI and disturbance. In the following section, neglecting for the time being additive disturbance effects, we provide a procedure for synthesizing these matrices with the aim to achieve *deterministic* ICI suppression, regardless of the multipath channel (so called *universal precoding*).

3. UNIVERSAL LINEAR PRECODING FOR FIR WL-ZF EQUALIZATION

In the absence of disturbance (i.e., $\tilde{\mathbf{v}}(n) = \mathbf{0}_P$), accounting for (5), the perfect or ZF symbol recovery condition $\mathbf{y}(n) = \mathbf{s}(n)$ leads to the linear matrix equation $\mathbf{g}\mathcal{H} = \mathbf{I}_M$ in the unknown \mathbf{g} , which is consistent (i.e., it admits at least one solution) if and only if the “augmented” matrix $\mathcal{H} \in \mathbb{C}^{2Q \times M}$ is full-column rank, that is, $\text{rank}(\mathcal{H}) = M$. It is noteworthy that since $2Q > M$ either in the ZP case or in the CP one, the matrix \mathcal{H} is tall by construction. Therefore, if $\text{rank}(\mathcal{H}) = M$, the ZF solution is *not* unique. Indeed, the general solution of $\mathbf{g}\mathcal{H} = \mathbf{I}_M$ can be written [12, 31] as

$$\mathbf{g}_{zf} = \underbrace{\mathcal{H}^\dagger}_{\mathbf{g}_{zf}^{(f)}} - \underbrace{\mathbf{y}\mathbf{\Pi}}_{\mathbf{g}_{zf}^{(a)}} = \mathbf{g}_{zf}^{(f)} - \mathbf{g}_{zf}^{(a)}, \quad (6)$$

where $\mathbf{g}_{zf}^{(f)} \in \mathbb{C}^{M \times 2Q}$ represents the minimum-norm (in the Frobenius sense) solution of $\mathbf{g}\mathcal{H} = \mathbf{I}_M$, the matrix $\mathbf{y} \in \mathbb{C}^{M \times (2Q-M)}$ is arbitrary, and $\mathbf{\Pi} \in \mathbb{C}^{(2Q-M) \times 2Q}$ is the *signal blocking matrix*, which is chosen so that the columns of $\mathbf{\Pi}^H$ constitute an orthonormal basis for $\mathcal{R}^\perp(\mathcal{H})$, that is, $\mathbf{\Pi}\mathcal{H} = \mathbf{O}_{(2Q-M) \times M}$ and $\mathbf{\Pi}\mathbf{\Pi}^H = \mathbf{I}_{2Q-M}$. In Section 4, we will show how to exploit the remaining free parameters, contained in \mathbf{y} , to mitigate the effects of the disturbance (NBI-plus-noise).³

³ It is worth noticing that the summands $\mathbf{g}_{zf}^{(f)}$ and $\mathbf{g}_{zf}^{(a)}$ are orthogonal, for any choice of \mathbf{y} , namely, $\mathbf{g}_{zf}^{(f)}[\mathbf{g}_{zf}^{(a)}]^H = \mathbf{O}_{M \times M}$. In this sense, the WL-ZF solution (6) can be regarded as a *generalized sidelobe canceler* (GSC) decomposition [19], which is well known in the array processing context.

Since the full-column rank property of \mathcal{H} is both a necessary and a sufficient condition for the existence of the FIR WL-ZF equalizer (6), the first step of our study consists of investigating whether the condition $\text{rank}(\mathcal{H}) = M$ is satisfied regardless of the underlying frequency-selective channel. In the ZP case, the rank properties of

$$\mathcal{H} = \mathcal{H}_{\text{zp}} \triangleq \begin{bmatrix} \mathbf{H}_{\text{zp}} \mathbf{F} \\ \mathbf{H}_{\text{zp}}^* \mathbf{F}^* \mathbf{J} \end{bmatrix} \in \mathbb{C}^{2P \times M} \quad (7)$$

are easily characterized, since the Toeplitz matrix \mathbf{H}_{zp} is full-column rank for any FIR channel of order L [1, 8, 9]. Indeed, owing to nonsingularity of \mathbf{F} and \mathbf{J} , it results that $\text{rank}(\mathbf{H}_{\text{zp}} \mathbf{F}) = \text{rank}(\mathbf{H}_{\text{zp}}^* \mathbf{F}^* \mathbf{J}) = \text{rank}(\mathbf{H}_{\text{zp}}) = M$. Henceforth, the augmented channel matrix \mathcal{H}_{zp} is *always* full-column rank and, thus, channel-irrespective WL-FIR perfect symbol recovery is possible. It is interesting to note that universal ZF symbol recovery is also guaranteed [1, 8, 9] for a ZP-based system by using a simpler L-FIR block equalizer, which can work either for proper or improper data symbols. However, as shown by our simulation results in Section 5, compared with its linear counterpart, a WL-ZF equalizer ensures much better performance in the presence of disturbance. As regards the choice of the nonsingular matrix \mathbf{F} , different universal precoders can be built. A simple choice, which is adopted in wireless OFDM systems, is the following:

$$\mathbf{F} = \mathbf{W}_{\text{IDFT}} \implies \tilde{\mathbf{F}}_{\text{IDFT}} \triangleq \mathbf{T}_{\text{zp}} \mathbf{W}_{\text{IDFT}}, \quad (8)$$

where $\{\mathbf{W}_{\text{IDFT}}\}_{mp} \triangleq (1/\sqrt{M})e^{j(2\pi/M)mp}$, for $m, p \in \{0, 1, \dots, M-1\}$, is the unitary symmetric IDFT matrix, and its inverse $\mathbf{W}_{\text{DFT}} \triangleq \mathbf{W}_{\text{IDFT}}^{-1} = \mathbf{W}_{\text{IDFT}}^*$ defines the DFT. In the CP case, the rank characterization of \mathcal{H} is less obvious than in the ZP one and, thus, is deferred to Section 3.1.

3.1. Full-column rank property of \mathcal{H} for a CP-based system

With reference to a CP-based system, let us study the rank properties of

$$\mathcal{H} = \mathcal{H}_{\text{cp}} \triangleq \begin{bmatrix} \mathbf{H}_{\text{cp}} \mathbf{F} \\ \mathbf{H}_{\text{cp}}^* \mathbf{F}^* \mathbf{J} \end{bmatrix} \quad (9)$$

whose characterization is more cumbersome than that of \mathcal{H}_{zp} , since, unlike \mathbf{H}_{zp} , the circulant matrix \mathbf{H}_{cp} turns out to be singular for some FIR channels. Preliminarily, observe that, by resorting to standard eigenstructure concepts [1, 32], one has $\mathbf{H}_{\text{cp}} = \mathbf{W}_{\text{IDFT}} \mathbf{A}_{\text{cp}} \mathbf{W}_{\text{DFT}}$, where the diagonal entries of $\mathbf{A}_{\text{cp}} \triangleq \text{diag}[\alpha_{\text{cp}}(0), \alpha_{\text{cp}}(1), \dots, \alpha_{\text{cp}}(M-1)] \in \mathbb{C}^{M \times M}$ are the values of the channel transfer function $H(z) \triangleq \sum_{\ell=0}^L h(\ell)z^{-\ell}$ evaluated at the subcarriers $z_m \triangleq e^{i(2\pi/M)m}$, that is, $\alpha_{\text{cp}}(m) = H(z_m)$, $\forall m \in \{0, 1, \dots, M-1\}$. Henceforth, one obtains from (7) that

$$\begin{aligned} \mathcal{H}_{\text{cp}} &= \underbrace{\begin{bmatrix} \mathbf{W}_{\text{IDFT}} & \mathbf{O}_{M \times M} \\ \mathbf{O}_{M \times M} & \mathbf{W}_{\text{IDFT}}^* \end{bmatrix}}_{\mathbf{W}_{\text{IDFT}} \in \mathbb{C}^{2M \times 2M}} \underbrace{\begin{bmatrix} \mathbf{A}_{\text{cp}} & \mathbf{O}_{M \times M} \\ \mathbf{O}_{M \times M} & \mathbf{A}_{\text{cp}}^* \end{bmatrix}}_{\mathbf{A}_{\text{cp}} \in \mathbb{C}^{2M \times 2M}} \underbrace{\begin{bmatrix} \mathbf{B}_{\text{cp}} \\ \mathbf{B}_{\text{cp}}^* \mathbf{J} \end{bmatrix}}_{\mathbf{B}_{\text{cp}} \in \mathbb{C}^{2M \times M}} \\ &= \mathbf{W}_{\text{IDFT}} \mathbf{A}_{\text{cp}} \mathbf{B}_{\text{cp}}, \end{aligned} \quad (10)$$

where we have defined the nonsingular matrix $\mathbf{B}_{\text{cp}} \triangleq \mathbf{W}_{\text{DFT}} \mathbf{F} \in \mathbb{C}^{M \times M}$, which will be referred to as the *frequency-domain precoding matrix*. As a first remark, note that, since \mathbf{W}_{IDFT} is nonsingular, it follows that $\text{rank}(\mathcal{H}_{\text{cp}}) = \text{rank}(\mathbf{A}_{\text{cp}} \mathbf{B}_{\text{cp}})$. Moreover, since \mathbf{B}_{cp} is nonsingular, the matrix \mathbf{B}_{cp} turns out to be full-column rank, that is, $\text{rank}(\mathbf{B}_{\text{cp}}) = M$. It is apparent that, contrary to the ZP case, nonsingularity of the (time-domain) precoding matrix \mathbf{F} or, equivalently, nonsingularity of the frequency-domain precoding matrix \mathbf{B}_{cp} , does not ensure by itself the full-column rank property of \mathcal{H}_{cp} , that is, the existence of FIR WL-ZF solutions. However, if $H(z)$ has no zeros on the subcarriers, that is, $\alpha_{\text{cp}}(m) \neq 0$, $\forall m \in \{0, 1, \dots, M-1\}$, it results that \mathbf{A}_{cp} is nonsingular and, consequently, $\text{rank}(\mathbf{A}_{\text{cp}} \mathbf{B}_{\text{cp}}) = \text{rank}(\mathbf{B}_{\text{cp}}) = M$. In other words, for a CP-based system, only if $H(z)$ has no zeros on the used subcarriers, the nonsingularity of the precoding matrix \mathbf{F} implies the full-column rank property of \mathcal{H}_{cp} . As a matter of fact, if \mathbf{A}_{cp} is nonsingular, the existence of ZF solutions is also guaranteed [1] for a CP-based system by using a simpler L-FIR block equalizer. However, the following theorem shows that, unlike L-FIR equalization, the presence of channel zeros on some subcarriers does not prevent perfect WL symbol recovery.

Theorem 1 (Rank characterization of \mathcal{H}_{cp}). *If the channel transfer function $H(z)$ has $0 \leq M_z \leq L$ distinct zeros on the subcarriers $z_{m_1} = e^{i(2\pi/M)m_1}, z_{m_2} = e^{i(2\pi/M)m_2}, \dots, z_{m_{M_z}} = e^{i(2\pi/M)m_{M_z}}$, with $m_1 \neq m_2 \neq \dots \neq m_{M_z} \in \{0, 1, \dots, M-1\}$, the augmented channel matrix \mathcal{H}_{cp} is full-column rank if and only if*

$$\text{rank}[(\mathbf{I}_{2M} - \mathcal{S}_z \mathcal{S}_z^T) \mathbf{B}_{\text{cp}}] = M, \quad (11)$$

where $\mathcal{S}_z \triangleq \text{diag}[\mathbf{S}_z, \mathbf{S}_z] \in \mathbb{R}^{2M \times 2M_z}$ and $\mathbf{S}_z \triangleq [\mathbf{1}_{m_1}, \mathbf{1}_{m_2}, \dots, \mathbf{1}_{m_{M_z}}] \in \mathbb{R}^{M \times M_z}$ are full-column rank matrices, with $\mathbf{1}_m$ denoting the $(m+1)$ th column of \mathbf{I}_M .

Proof. See Appendix A. \square

First of all, it should be observed that Theorem 1 generalizes the results of [20], which are targeted at nonredundant precoding, to the more general case of CP-based redundant precoders. Theorem 1 should be good news to system designers since it states that, for a CP-based transmission, perfect WL symbol recovery is possible even when the channel transfer function has zeros on the used subcarriers, that is, $M_z \neq 0$. In this case, however, the condition to be fulfilled is that the matrix $(\mathbf{I}_{2M} - \mathcal{S}_z \mathcal{S}_z^T) \mathbf{B}_{\text{cp}} \in \mathbb{C}^{2M \times M}$ must be full-column rank. It can be verified by direct inspection that all the $2M_z$ rows of $(\mathbf{I}_{2M} - \mathcal{S}_z \mathcal{S}_z^T) \mathbf{B}_{\text{cp}}$ located in the positions

$$\begin{aligned} \mathcal{I}_{m_1, m_2, \dots, m_{M_z}} &\triangleq \{m_1 + 1, m_2 + 1, \dots, m_{M_z} + 1, \\ &\quad m_1 + M + 1, m_2 + M + 1, \dots, m_{M_z} + M + 1\} \end{aligned} \quad (12)$$

are zero (all the entries are equal to zero), whereas the $2(M - M_z)$ remaining ones coincide with the corresponding rows of \mathbf{B}_{cp} . Consequently, fulfillment of condition (11) necessarily requires that $2(M - M_z) \geq M$, which imposes that the number of subcarriers must be greater than or equal to $2M_z$, that

is, $M \geq 2M_z$. In the worst case when $M_z = L$, that is, all the channel zeros are located at the subcarriers, the minimum number of subcarriers is equal to $2L$. This is a very mild condition, which is satisfied by many systems of practical interest. Besides the channel-zero configuration, the existence of FIR WL-ZF solutions depends on the precoding strategy employed at the transmitter. It is interesting to consider the case of an IDFT precoding, that is, $\mathbf{F} = \mathbf{W}_{\text{IDFT}}$, which is the precoder considered in [12]. We recall that this kind of precoding, typically used in OFDM wireless systems, is universal for both **L** and WL-FIR perfect symbol recovery in ZP-based systems. In this case, it results that $\mathbf{B}_{\text{cp}} = \mathbf{I}_M$ and, hence, one has

$$\mathcal{B}_{\text{cp}} = \begin{bmatrix} \mathbf{I}_M \\ \mathbf{J} \end{bmatrix}. \quad (13)$$

Let $M \geq 2M_z$, it is readily verified that, when \mathcal{B}_{cp} assumes the form given by (13), the matrix $(\mathbf{I}_{2M} - \mathcal{G}_z \mathcal{G}_z^T) \mathcal{B}_{\text{cp}}$ has rank equal to $M - M_z$, for any $\{m_1, m_2, \dots, m_{M_z}\} \subset \{0, 1, \dots, M - 1\}$. In other words, as in the case of FIR L-ZF equalization, when an IDFT precoding is used, perfect WL-FIR symbol recovery is possible in a CP-based system if and only if the channel transfer function has no zeros on the used subcarriers, that is, $M_z = 0$. This result is in accordance with [12, Lemma 2].

Theorem 1 evidences that, in contrast with ZP-based systems, even when the frequency-domain precoding matrix \mathbf{B}_{cp} is nonsingular, the full-column rank property of \mathcal{H}_{cp} explicitly depends on the presence of channel zeros located at the subcarriers $\{z_m\}_{m=0}^{M-1}$, whose number M_z and locations m_1, m_2, \dots, m_{M_z} are *unknown* at the receiver. Remarkably, Theorem 1 additionally allows us to provide *universal* code designs, which assure that \mathcal{H}_{cp} is full-column rank for *any* possible configuration of the channel zeros. First of all, we observe that, although M_z is unknown, it is upper bounded by L , that is, $0 \leq M_z \leq L$. Thus, by virtue of Theorem 1, we can infer that the augmented matrix \mathcal{H}_{cp} is full-column rank for any FIR channel of order (smaller than or equal to) L if and only if

$$\begin{aligned} \text{rank}[(\mathbf{I}_{2M} - \mathcal{G}_{\text{univ}} \mathcal{G}_{\text{univ}}^T) \mathcal{B}_{\text{cp}}] \\ = M, \quad \forall \{m_1, m_2, \dots, m_L\} \subset \{0, 1, \dots, M - 1\}, \end{aligned} \quad (14)$$

where $\mathcal{G}_{\text{univ}} \triangleq \text{diag}[\mathbf{S}_{\text{univ}}, \mathbf{S}_{\text{univ}}] \in \mathbb{R}^{2M \times 2L}$ and $\mathbf{S}_{\text{univ}} \triangleq [\mathbf{I}_{m_1}, \mathbf{I}_{m_2}, \dots, \mathbf{I}_{m_L}] \in \mathbb{R}^{M \times L}$ are full-column rank matrices. Condition (14) necessarily requires that $M \geq 2L$. Relying on the fact that the matrix $(\mathbf{I}_{2M} - \mathcal{G}_{\text{univ}} \mathcal{G}_{\text{univ}}^T) \mathcal{B}_{\text{cp}}$ is obtained from \mathcal{B}_{cp} by setting to zero all the entries of its $2L$ rows located in the positions $\mathcal{J}_{m_1, m_2, \dots, m_L}$ (see (12) with $M_z = L$), we can state the following necessary and sufficient condition for universal precoding design.

Condition U_{cp} (universal precoding for CP-based systems)

Let $\zeta_m^T \triangleq [\zeta_1^{(m)}, \zeta_2^{(m)}, \dots, \zeta_J^{(m)}] \in \mathbb{C}^{1 \times M}$ denote the $(m + 1)$ th row of $\mathbf{B}_{\text{cp}} = \mathbf{W}_{\text{DFT}} \mathbf{F}$, with $m \in \{0, 1, \dots, M - 1\}$; when $M \geq 2L$, for any subset of distinct indices $\{m_1, m_2, \dots, m_{M-L}\} \subset \{0, 1, \dots, M - 1\}$, there exists M linearly independent vectors from the total set $\{\zeta_{m_1}, \zeta_{m_2}, \dots, \zeta_{m_{M-L}}, \mathbf{J}\zeta_{m_1}^*, \mathbf{J}\zeta_{m_2}^*, \dots, \mathbf{J}\zeta_{m_{M-L}}^*\}$.

Condition U_{cp} shows that channel-irrespective FIR WL-ZF equalization is possible not only in a ZP-based system, but also in a CP-based one. It is worthwhile to observe that condition U_{cp} does not uniquely specify \mathbf{B}_{cp} (or, equivalently, \mathbf{F}) and, thus, different universal precoders can be built. For instance, condition U_{cp} can be satisfied by imposing that each row of \mathbf{B}_{cp} be a Vandermonde-like vector. Specifically, let us select $M \geq 2L$ nonzero numbers $\{\rho_m\}_{m=0}^{M-1}$ and build the vectors ζ_m as

$$\zeta_m = \frac{1}{\sqrt{\chi_m}} [1, \rho_m, \rho_m^2, \dots, \rho_m^{M-1}]^T, \quad \forall m \in \{0, 1, \dots, M - 1\}, \quad (15)$$

where normalization by $1/\sqrt{\chi_m}$ has been introduced to ensure that $\|\zeta_m\|^2 = 1$, which in its turn implies that $\text{trace}(\mathbf{F}^H \mathbf{F}) = M$. In this case, it is important to observe that $\mathbf{J}\zeta_m^*$ is again a Vandermonde-like vector, since it follows that

$$\begin{aligned} \mathbf{J}\zeta_m^* = \frac{1}{\sqrt{\chi_m}} [1, (\rho_m^* e^{j2\pi\beta}), (\rho_m^* e^{j2\pi\beta})^2, \dots, (\rho_m^* e^{j2\pi\beta})^{M-1}]^T, \\ \forall m \in \{0, 1, \dots, M - 1\}. \end{aligned} \quad (16)$$

Relying on the properties of Vandermonde vectors [32], it is not difficult to prove that condition U_{cp} is satisfied if one imposes the following two conditions:

- (C1) $\rho_\ell \neq \rho_m, \forall \ell, m \in \{0, 1, \dots, M - 1\}$;
- (C2) $\rho_\ell \neq \rho_m^* e^{j2\pi\beta}, \forall \ell, m \in \{0, 1, \dots, M - 1\}$.

Condition (C1) imposes that the numbers $\rho_0, \rho_1, \dots, \rho_{M-1}$ be distinct; this assures that the sets of vectors $\{\zeta_{m_1}, \zeta_{m_2}, \dots, \zeta_{m_{M-L}}\}$ and $\{\mathbf{J}\zeta_{m_1}^*, \mathbf{J}\zeta_{m_2}^*, \dots, \mathbf{J}\zeta_{m_{M-L}}^*\}$ are linearly independent. In addition, condition (C2) imposes that, given the linearly independent set $\{\zeta_{m_1}, \zeta_{m_2}, \dots, \zeta_{m_{M-L}}\}$, the extended set of vectors, obtained by adding the linearly independent vectors $\mathbf{J}\zeta_{m_1}^*, \mathbf{J}\zeta_{m_2}^*, \dots, \mathbf{J}\zeta_{m_{M-L}}^*$, is again linearly independent. Observe that, if the numbers ζ_m are chosen equispaced on the unit circle, by setting $\rho_m = e^{-j(2\pi/M)m}, \forall m \in \{0, 1, \dots, M - 1\}$, one obtains a DFT frequency-domain precoding, that is, $\mathbf{B}_{\text{cp}} = \mathbf{W}_{\text{DFT}}$, which leads to an identity time-domain precoder, that is, $\mathbf{F} = \mathbf{W}_{\text{IDFT}} \mathbf{B}_{\text{cp}} = \mathbf{I}_M$. Such a precoder is not universal since the numbers $\{e^{-j(2\pi/M)m}\}_{m=0}^{M-1}$ fulfill condition (C1) but do not satisfy condition (C2); indeed, in this case, condition (C2) ends up to the following one:

$$\frac{\ell + m}{M} + \beta \neq h, \quad \forall \ell, m \in \{0, 1, \dots, M - 1\}, \forall h \in \mathbb{Z} \quad (17)$$

which is violated either when $\beta = 0$ or when $\beta = 1/2$. A similar result holds for an IDFT frequency-domain precoding, that is, when $\rho_m = e^{j(2\pi/M)m}, \forall m \in \{0, 1, \dots, M - 1\}$. To obtain a set of M complex-valued parameters $\{\rho_m\}_{m=0}^{M-1}$ equispaced on the unit circle, which satisfy condition (C2), it is sufficient to introduce a suitable rotation by setting $\rho_m = e^{-j((2\pi/M)m - \theta)}, \forall m \in \{0, 1, \dots, M - 1\}$ and $\theta \in (0, 2\pi)$. In this latter case, the frequency-domain precoding matrix assumes the form $\mathbf{B}_{\text{cp}} = \mathbf{W}_{\text{DFT}} \mathbf{\Theta}$, where $\mathbf{\Theta} \triangleq$

$\text{diag}[1, e^{j\theta}, e^{j2\theta}, \dots, e^{j(M-1)\theta}] \in \mathbb{C}^{M \times M}$, which leads to the time-domain precoding matrix

$$\mathbf{F} = \mathbf{W}_{\text{IDFT}} \mathbf{B}_{\text{CP}} = \mathbf{\Theta} \implies \tilde{\mathbf{F}}_{\text{RMIC}} \triangleq \mathbf{T}_{\text{CP}} \mathbf{\Theta}, \quad (18)$$

which will be referred to as *redundant modulation-induced cyclostationarity* (RMIC) precoder. To fulfill condition (C2), the angle rotation θ must obey the condition

$$\begin{aligned} \theta &\neq \frac{\pi}{M}(\ell + m) + \pi\beta + h\pi, \\ \forall \ell, m \in \{0, 1, \dots, M-1\}, \forall h \in \mathbb{Z}. \end{aligned} \quad (19)$$

The precoder specified by (18)-(19) satisfies condition U_{CP} and, hence, it represents a *first* simple example of precoding ensuring universal WL perfect symbol recovery in CP-based systems. It is important to observe that MIC precoding techniques were originally proposed [35, 36] for nonredundantly precoded systems. In comparison with redundant precoding techniques, the drawback of nonredundant MIC-based approaches is the lack of FIR L-ZF equalizers for FIR channels. As shown in [20], such a shortcoming can be avoided by resorting to WL-FIR block processing at the receiver.

Finally, a remark regarding computational complexity **2** **issue** for both the ZP and CP cases is in order. For a ZP-based system, the synthesis of the WL-ZF equalizer (6) requires evaluation of $\mathcal{G}_{\text{zf}}^{(f)}$, which turns out to be equal to $\mathcal{H}_{\text{zp}}^\dagger = (\mathcal{H}_{\text{zp}}^H \mathcal{H}_{\text{zp}})^{-1} \mathcal{H}_{\text{zp}}^H$. Therefore, in this case, the computational complexity of the minimum-norm WL-ZF equalizer is essentially dominated by the inversion of the $M \times M$ matrix $\mathcal{H}_{\text{zp}}^H \mathcal{H}_{\text{zp}}$, which cannot be precomputed offline, since the matrix to be inverted depends on the channel impulse response. A similar problem also arises in the case of FIR L-ZF equalization for ZP-based systems [10], where the pseudoinverse of \mathbf{H}_{zp} has to be evaluated, which again involves inversion of an $M \times M$ matrix. On the other hand, for a CP-based system, synthesis of the WL-ZF equalizer (6) requires evaluation of $\mathcal{G}_{\text{zf}}^{(f)}$, which is given by $\mathcal{H}_{\text{cp}}^\dagger = (\mathcal{A}_{\text{cp}} \mathcal{B}_{\text{cp}})^\dagger \mathcal{W}_{\text{DFT}} = (\mathcal{B}_{\text{cp}}^H \mathcal{A}_{\text{cp}}^H \mathcal{A}_{\text{cp}} \mathcal{B}_{\text{cp}})^{-1} \mathcal{B}_{\text{cp}}^H \mathcal{A}_{\text{cp}}^H \mathcal{W}_{\text{DFT}}$, where $\mathcal{W}_{\text{DFT}} \triangleq \mathcal{W}_{\text{IDFT}}^*$. Similar to the ZP case, inversion of the $M \times M$ matrix $\mathcal{B}_{\text{cp}}^H \mathcal{A}_{\text{cp}}^H \mathcal{A}_{\text{cp}} \mathcal{B}_{\text{cp}}$ cannot be precomputed offline since the matrix to be inverted depends on the channel transfer function. Roughly speaking, evaluation of the minimum-norm WL-ZF equalizer approximately requires the same computational burden in either the ZP or the CP case. However, CP precoding is fully compatible with existing MC-based standards (e.g., IEEE 802.11a and HIPERLAN/2) and involves a smaller power backoff than ZP transmission techniques [10].

4. WL-ZF MMOE DISTURBANCE MITIGATION

The unified form (6) of the WL-ZF equalizer, which encompasses both ZP- and CP-based systems, shows the existence of free parameters, embodied in matrix \mathcal{Y} , which can be exploited for further optimization in the presence of disturbance. Towards this aim, the matrix \mathcal{Y} is chosen here so as to minimize the mean-output-energy (MOE) at the output of

the WL-ZF equalizer, which, by substituting (6) in (5), can be written as

$$\mathbf{y}(n) = \mathcal{G}_{\text{zf}} \mathcal{H} \mathbf{s}(n) + \mathcal{G}_{\text{zf}} \mathbf{d}(n) = \mathbf{s}(n) + (\mathcal{G}_{\text{zf}}^{(f)} - \mathcal{Y} \mathbf{\Pi}) \mathbf{d}(n). \quad (20)$$

Therefore, mitigation of the disturbance contribution at the equalizer output amounts to choosing \mathcal{Y} as the solution of the following *unconstrained* quadratic optimization problem:

$$\mathcal{Y}_{\text{mmoe}} = \arg \min_{\mathcal{Y} \in \mathbb{C}^{M \times (2Q-M)}} E \left[\left\| (\mathcal{G}_{\text{zf}}^{(f)} - \mathcal{Y} \mathbf{\Pi}) \mathbf{d}(n) \right\|^2 \right], \quad (21)$$

whose solution is given [12] by

$$\mathcal{Y}_{\text{mmoe}} = \mathcal{G}_{\text{zf}} \mathbf{R}_{\text{dd}} \mathbf{\Pi}^H (\mathbf{\Pi} \mathbf{R}_{\text{dd}} \mathbf{\Pi}^H)^{-1}, \quad (22)$$

where $\mathbf{R}_{\text{dd}} \triangleq E[\mathbf{d}(n) \mathbf{d}^H(n)] \in \mathbb{C}^{2Q \times 2Q}$ is the autocorrelation matrix of the augmented disturbance vector $\mathbf{d}(n)$. By substituting (22) in (6), the WL-ZF-MMOE equalizer is explicitly characterized by

$$\mathcal{G}_{\text{zf-mmoe}} = \mathcal{G}_{\text{zf}}^{(f)} - \mathcal{Y}_{\text{mmoe}} \mathbf{\Pi}, \quad (23)$$

and, after some straightforward algebraic manipulations, the corresponding (minimum) mean-output-energy of the disturbance is given by

$$\begin{aligned} \mathcal{P}_{\text{d,min}} &\triangleq E \left[\left\| (\mathcal{G}_{\text{zf}}^{(f)} - \mathcal{Y}_{\text{mmoe}} \mathbf{\Pi}) \mathbf{d}(n) \right\|^2 \right] \\ &= \text{trace} \left[\mathcal{G}_{\text{zf}}^{(f)} \mathbf{R}_{\text{dd}} (\mathcal{G}_{\text{zf}}^{(f)})^H \right] \\ &\quad - \text{trace} \left[\mathcal{G}_{\text{zf}}^{(f)} \mathbf{R}_{\text{dd}} \mathbf{\Pi}^H (\mathbf{\Pi} \mathbf{R}_{\text{dd}} \mathbf{\Pi}^H)^{-1} \mathbf{\Pi} \mathbf{R}_{\text{dd}} (\mathcal{G}_{\text{zf}}^{(f)})^H \right]. \end{aligned} \quad (24)$$

Synthesis of the WL-ZF-MMOE equalizer (23) requires the disturbance autocorrelation matrix \mathbf{R}_{dd} to be consistently estimated from the augmented version $\mathbf{z}(n) \in \mathbb{C}^{2Q}$ of the IBI-free received vector $\mathbf{r}(n) \triangleq \mathbf{R} \tilde{\mathbf{r}}(n) \in \mathbb{C}^Q$, which, accounting for (1) and (5), assumes the form

$$\mathbf{z}(n) \triangleq \begin{bmatrix} \mathbf{r}(n) \\ \mathbf{r}^*(n) \end{bmatrix} = \mathcal{H} \mathbf{s}(n) + \underbrace{\begin{bmatrix} \mathbf{v}(n) \\ \mathbf{v}^*(n) \end{bmatrix}}_{\mathbf{d}(n)} = \mathcal{H} \mathbf{s}(n) + \mathbf{d}(n), \quad (25)$$

with $\mathbf{v}(n) \triangleq \mathbf{R} \tilde{\mathbf{v}}(n) \in \mathbb{C}^Q$. The estimate of \mathbf{R}_{dd} is complicated by the fact that $\mathbf{z}(n)$ contains also the contribution of the MC signal. However, the WL-ZF-MMOE equalizer can also be expressed in terms of the autocorrelation matrix of $\mathbf{z}(n)$, which, under assumptions (A1) and (A2), is given by

$$\mathbf{R}_{\text{zz}} \triangleq E[\mathbf{z}(n) \mathbf{z}^H(n)] = \sigma_s^2 \mathcal{H} \mathcal{H}^H + \mathbf{R}_{\text{dd}}. \quad (26)$$

By virtue of the signal blocking property of $\mathbf{\Pi}$, it results that $\mathbf{\Pi} \mathbf{R}_{\text{zz}} = \mathbf{\Pi} \mathbf{R}_{\text{dd}}$. Consequently, the solution (22) of the optimization problem (21) can be equivalently written as

$$\mathcal{Y}_{\text{mmoe}} = \mathcal{G}_{\text{zf}} \mathbf{R}_{\text{zz}} \mathbf{\Pi}^H (\mathbf{\Pi} \mathbf{R}_{\text{zz}} \mathbf{\Pi}^H)^{-1}, \quad (27)$$

where the matrix \mathbf{R}_{zz} can be estimated from the received data more easily than \mathbf{R}_{dd} .

The aim of this section is to provide a theoretical analysis of the NBI suppression capabilities of the WL-ZF-MMOE equalizer given by (23), whose merits have experimentally been tested in [12] with reference only to a CP-based system with IDFT precoding. To this end, we recall that $\mathbf{v}(n)$ is composed of two terms $\mathbf{v}(n) = \mathbf{v}_{\text{nbi}}(n) + \mathbf{v}_{\text{noise}}(n)$, where $\mathbf{v}_{\text{nbi}}(n)$ and $\mathbf{v}_{\text{noise}}(n)$ account for NBI and noise, respectively. In addition to assumption (A2), we assume that

- (A3) the first $R_{\text{nbi}} \ll Q$ eigenvalues of the NBI autocorrelation matrix $\mathbf{R}_{\text{nbi}} \triangleq E[\mathbf{v}_{\text{nbi}}(n)\mathbf{v}_{\text{nbi}}^H(n)]$ are significantly different from zero, whereas the remaining ones are vanishingly small;
- (A4) the vector $\mathbf{v}_{\text{noise}}(n)$ is a white random process, statistically independent of $\mathbf{v}_{\text{nbi}}(n)$, with autocorrelation matrix $\mathbf{R}_{\text{noise}} \triangleq E[\mathbf{v}_{\text{noise}}(n)\mathbf{v}_{\text{noise}}^H(n)] = \sigma_v^2 \mathbf{I}_Q$.

It is worth noticing that, by invoking some results [37] regarding the approximate dimensionality of exactly time-limited and nominally band-limited signals, assumption (A3) is well verified for reasonably large values of Q , with $R_{\text{nbi}} = \lceil QT_c W_{\text{nbi}} \rceil + 1$, where W_{nbi} is the (nominal) bandwidth of the continuous-time NBI process. In the case of NBI, it happens in practice that, compared with the bandwidth of the MC system, the bandwidth W_{nbi} is significantly smaller, that is, $T_c W_{\text{nbi}} \ll 1$, and, thus, it turns out that $R_{\text{nbi}} \ll Q$. Under assumption (A3), the NBI autocorrelation matrix can be well modeled by the following full-rank factorization (see [38]) $\mathbf{R}_{\text{nbi}} = \mathbf{L}\mathbf{L}^H$, where the matrix $\mathbf{L} \in \mathbb{C}^{Q \times R_{\text{nbi}}}$ is full-column rank, that is, $\text{rank}(\mathbf{L}) = R_{\text{nbi}}$. By virtue of assumptions (A2), (A3), and (A4), the autocorrelation matrix of the augmented disturbance vector $\mathbf{d}(n)$ can be expressed as

$$\mathbf{R}_{dd} = \mathcal{L}\mathcal{L}^H + \sigma_v^2 \mathbf{I}_{2Q}, \quad (28)$$

where

$$\mathcal{L} \triangleq \begin{bmatrix} \mathbf{L} & \mathbf{O}_{Q \times R_{\text{nbi}}} \\ \mathbf{O}_{Q \times R_{\text{nbi}}} & \mathbf{L}^* \end{bmatrix} \in \mathbb{C}^{2Q \times 2R_{\text{nbi}}} \quad (29)$$

is a full-column rank matrix. As a first remark, it is interesting to observe that, in the absence of NBI, that is, $\mathbf{L} = \mathbf{O}_{Q \times R_{\text{nbi}}}$, it results that $\mathbf{R}_{dd} = \sigma_v^2 \mathbf{I}_{2Q}$, which can be substituted in (22), thus obtaining

$$\mathcal{Y}_{\text{mmoe}} = \mathcal{G}_{\text{zf}} \mathbf{\Pi}^H = \mathbf{O}_{M \times (2Q-M)}, \quad (30)$$

where the second equality is a consequence of the fact that $\mathbf{\Pi}\mathcal{H} = \mathbf{O}_{(2Q-M) \times M}$. Henceforth, in the absence of NBI, the WL-ZF-MMOE equalizer (23) boils down to the minimum-norm solution $\mathcal{G}_{\text{zf}}^{(f)} = \mathcal{H}^\dagger$ of the ZF matrix equation $\mathcal{G}\mathcal{H} = \mathbf{I}_M$. The following theorem characterizes the NBI suppression capability of the WL-ZF-MMOE equalizer, in the high signal-to-noise ratio (SNR) regime, by evaluating the disturbance mean-output-energy $\mathcal{P}_{d,\text{min}}$ as σ_v^2 approaches to zero.

Theorem 2 (NBI suppression analysis). *Assume that the following conditions hold:*

- (C3) $2Q - M \geq 2R_{\text{nbi}}$;
- (C4) \mathcal{H} is full-column rank, that is, $\text{rank}(\mathcal{H}) = M$;
- (C5) $\mathcal{R}(\mathcal{H}) \cap \mathcal{R}(\mathcal{L}) = \{\mathbf{0}_{2Q}\}$.

In the limiting case of vanishingly small noise, the WL-ZF-MMOE equalizer (23) assures perfect NBI suppression, that is, $\lim_{\sigma_v^2 \rightarrow 0} \mathcal{P}_{d,\text{min}} = 0$.

Proof. See Appendix B. \square

It is noteworthy that the proof of **Theorem 2** is similar in spirit with that reported in [13, 15] in the case of a CP-based system employing linear block equalization, moreover it allows one to obtain clear insights about the effects of system parameters on the performance of the WL-ZF-MMOE equalizer. Specifically, for a ZP-based system ($Q = P$), condition (C3) assumes the form

$$R_{\text{nbi}} \leq \frac{M}{2} + L, \quad (31)$$

whereas, for a CP-based system ($Q = M$), it becomes

$$R_{\text{nbi}} \leq \frac{M}{2}. \quad (32)$$

Thus, in both cases, condition (C3) poses an upper bound on the rank R_{nbi} (i.e., the bandwidth W_{nbi}) of the NBI signal to be rejected. Roughly speaking, condition (32) means that, when employed in a CP-based system, the WL-ZF-MMOE equalizer is able to suppress NBI signals whose bandwidth W_{nbi} can be as wide as half the bandwidth of the MC signal, provided that conditions (C4) and (C5) are fulfilled. Observe that, in the case of linear ZF equalization, when all the M subcarriers are used (i.e., there are no virtual carriers) and complete CP removal is performed at the receiver, perfect NBI suppression cannot be achieved with the L-ZF-MMOE equalizer [13], even in the absence of noise. On the other hand, comparing (31) with (32), when employed in a ZP-based system, it is seen that the WL-ZF-MMOE equalizer can completely reject, in the high SNR region, interfering signals with a wider bandwidth than in the CP case. This result stems from the fact that ZP precoding performs IBI suppression without discarding any portion of the received signal, that is, without decreasing the dimensionality of the observation space as in the CP case. Condition (C4) has been deeply discussed in Section 3. Finally, condition (C5) is a pure technical condition, which is not easily interpretable. It essentially imposes that the two subspaces $\mathcal{R}(\mathcal{H})$ and $\mathcal{R}(\mathcal{L})$ must be *nonoverlapping* or *disjoint*, which is less restrictive [39] than simple orthogonality between the same subspaces. On the basis of our simulation results, we can state that, if conditions (C3) and (C4) hold, it is very unlikely that condition (C5) is violated in practice.

5. SIMULATION RESULTS

In this section, we present Monte Carlo computer simulations aimed at corroborating the theoretical results provided in Sections 3 and 4. In all the experiments, the following simulation setting is assumed. The CP- and ZP-based MC systems employ OQPSK improper signaling. Both systems use

two different precoding strategies: (i) the IDFT precoder, that is, $\mathbf{F} = \mathbf{W}_{\text{IDFT}}$; (ii) the RMIC precoder, that is, $\mathbf{F} = \mathbf{\Theta}$, with $\theta = \pi/32$. The discrete-time NBI signal $\tilde{v}_{\text{nbi}}(n) \triangleq \tilde{v}_{c,\text{nbi}}(nT_c)$ is modeled as a Gaussian random process, with autocorrelation function

$$r_{\text{nbi}}(m) \triangleq \mathbb{E}[\tilde{v}_{\text{nbi}}(n)\tilde{v}_{\text{nbi}}^*(n-m)] = \sigma_{\text{nbi}}^2 a^{|m|} e^{j2\pi m \nu_0}, \quad (33)$$

where σ_{nbi}^2 is the NBI power, ν_0 is the NBI carrier frequency-offset and, after some straightforward calculations, a can be related to the 3-dB NBI bandwidth by

$$W_{\text{nbi}} = \frac{1}{2\pi} \arccos\left(\frac{4a - a^2 - 1}{2a}\right), \quad 0.172 \leq a < 1. \quad (34)$$

The parameters a and ν_0 are set to 0.99 (corresponding to $W_{\text{nbi}} \approx 0.0016$) and $3.5/M$, respectively. The SNR is defined as⁴

$$\text{SNR} \triangleq \frac{\sigma_s^2 \text{trace}(\tilde{\mathbf{F}}\tilde{\mathbf{F}}^H)}{M\sigma_w^2} \quad (35)$$

and, unless otherwise specified, is set to 20 dB. The SIR is defined as

$$\text{SIR} \triangleq \frac{\sigma_s^2 \text{trace}(\tilde{\mathbf{F}}\tilde{\mathbf{F}}^H)}{M\sigma_{\text{nbi}}^2} \quad (36)$$

and, unless otherwise specified, is set to 10 dB. All the considered equalizers⁵ are synthesized by assuming perfect knowledge of both the channel and the autocorrelation matrix of the disturbance vector.⁶ Finally, as performance measure, we adopt the average bit-error rate (ABER), defined as $\text{ABER} \triangleq (1/M) \sum_{m=0}^{M-1} \text{BER}_m$, where BER_m is the output bit-error rate (BER) at the m th subcarrier. For each Monte Carlo run (wherein, besides the channel impulse response, independent sets of noise, NBI and data sequences were randomly generated), an independent record of $K_{\text{aber}} = 10^4$ MC symbols, which correspond to $(M \cdot K_{\text{aber}})$ OQPSK symbols, was considered to evaluate the ABER.

⁴ Herein, the SNR is defined as the ratio between the average energy per symbol $\mathbb{E}[\|\tilde{\mathbf{u}}(n)\|^2]/M = [\sigma_s^2 \text{trace}(\tilde{\mathbf{F}}\tilde{\mathbf{F}}^H)]/M$ expended by the transmitter and the noise variance σ_w^2 , and it should not be confused with the SNR at the receiver input.

⁵ In the sequel, for notational convenience, a particular equalizer, which operates in a system employing a given precoding technique, will be synthetically referred to through the acronym of the equalizer followed by the acronym of the precoder enclosed in round brackets, for example, the notation “WL-ZF-MMOE (IDFT)” means that the WL-ZF-MMOE equalizer is used at the receiver and, at the same time, IDFT precoding is employed at the transmitter.

⁶ With reference to linear processing, it is theoretically shown in [13] that, when the second-order statistics of the received data are estimated on the basis of a finite sample size, the L-ZF-MMOE equalizer turns out to be considerably robust against estimation errors. A similar analysis and conclusion can be also inferred for the WL counterpart of the L-ZF-MMOE receiver.

5.1. Environment 1: MC system employing $M = 16$ subcarriers with ZP/CP length $L_r = 3$

In this environment, the CP- and ZP-based MC systems employ $M = 16$ subcarriers, with $L_r = 3$. Observe that, in this case, it results that $W_{\text{nbi}} \approx 0.025/M$, that is, the NBI bandwidth is about 2.5% of the subcarrier spacing. The baseband discrete-time multipath channel $\{h(m)\}_{m=0}^L$ is a random FIR filter of order $L = 3$, whose transfer function is given by

$$H(z) = (1 - \zeta_1 z^{-1})(1 - \zeta_2 z^{-1})(1 - \zeta_3 z^{-1}), \quad (37)$$

where the group $(\zeta_1, \zeta_2, \zeta_3)$ of its three zeros assumes a different configuration in each Monte Carlo run. During the first 16 runs, we set $\zeta_1 = e^{i(2\pi/M)m_1}$ (one zero on the subcarriers), where, in each run, m_1 takes on a different value in $\{0, 1, \dots, M-1\}$, whereas the magnitudes and phases of ζ_2 and ζ_3 , which are modeled as mutually independent random variables uniformly distributed over the intervals $(0, 2)$ and $(0, 2\pi)$, respectively, are randomly and independently generated from run to run. During the subsequent $\binom{16}{2} = 120$ runs, we set $\zeta_1 = e^{i(2\pi/M)m_1}$ and $\zeta_2 = e^{i(2\pi/M)m_2}$ (two zeros on the subcarriers), where, in each run, m_1 and m_2 take on a different value in $\{0, 1, \dots, M-1\}$, with $m_1 \neq m_2$, whereas the magnitude and phase of ζ_3 , which are modeled as mutually independent random variables uniformly distributed over the intervals $(0, 2)$ and $(0, 2\pi)$, respectively, are randomly and independently generated from run to run. During the last $\binom{16}{3} = 560$ runs, we set $\zeta_1 = e^{i(2\pi/M)m_1}$, $\zeta_2 = e^{i(2\pi/M)m_2}$, and $\zeta_3 = e^{i(2\pi/M)m_3}$ (three zeros on the subcarriers), where, in each run, m_1 , m_2 , and m_3 take on a different value in $\{0, 1, \dots, M-1\}$, with $m_1 \neq m_2 \neq m_3$. In this way, one obtains $16 + 120 + 560 = 696$ independent channel realizations and, thus, 696 Monte Carlo runs.

5.1.1. ABER versus SNR

In this experiment, we evaluated the performances of the considered equalizers as a function of the SNR ranging from 0 to 30 dB. In Figure 2, we considered a CP-based system performing either linear⁷ or WL block processing at the receiver. In this case, it is apparent from Figure 2 that the curves of the “L-ZF (RMIC),” “L-ZF (IDFT),” and “WL-ZF-MMOE (IDFT)” equalizers level off in the high SNR region, which is the natural consequence of the fact that these receivers do not ensure perfect ICI and NBI suppression when the channel transfer function exhibits zeros located on the subcarriers. On the other hand, when the RMIC precoding is used, perfect WL symbol recovery in the absence of noise is guaranteed regardless of the channel zero locations. In fact, the “WL-ZF-MMOE (RMIC)” equalizer exhibits satisfactory ICI suppression capabilities, as well as a strong robustness against

⁷ When complete CP removal is performed at the receiver, the ZF constraint leads to a unique solution irrespectively of the adopted precoding strategy; in this case, hence, the L-ZF equalizer cannot be further optimized (e.g., in the MMOE sense).

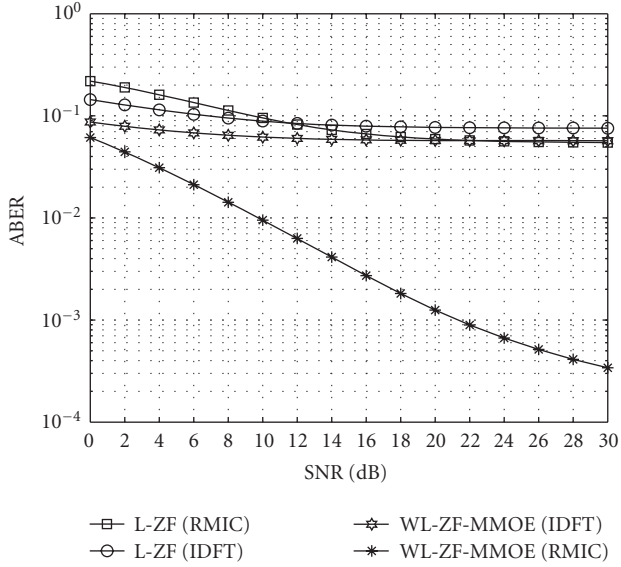


FIGURE 2: ABER versus SNR (Environment 1, CP-based system, SIR = 10 dB).

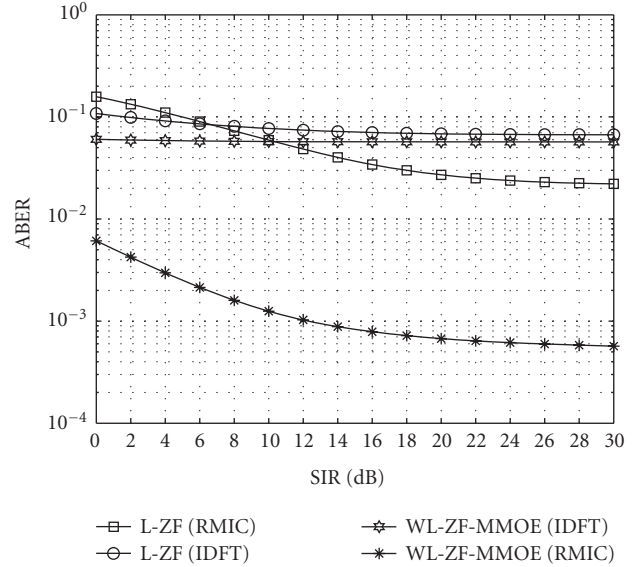


FIGURE 4: ABER versus SIR (Environment 1, CP-based system, SNR = 20 dB).

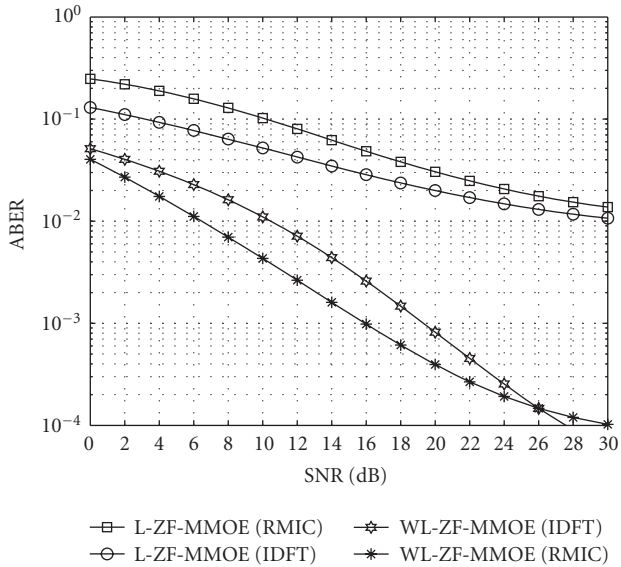


FIGURE 3: ABER versus SNR (Environment 1, ZP-based system, SIR = 10 dB).

NBI, assuring in particular a huge performance gain with respect to the “WL-ZF-MMOE (IDFT)” receiver.

The results of Figure 3 were obtained instead by considering a ZP-based system. In this scenario, both IDFT and RMIC precoding assure the existence of L- and WL-ZF solutions for any FIR channel of order less than or equal to L . It can be seen that, notwithstanding their channel-irrespective ICI suppression capabilities, the “L-ZF-MMOE (RMIC)” and “L-ZF-MMOE (IDFT)” equalizers are not able to achieve satisfactory NBI rejection, achieving ABER of only about 10^{-2} for SNR = 30 dB. In contrast, both the “WL-ZF-MMOE (IDFT)” and “WL-ZF-MMOE (RMIC)” equal-

izers not only assure perfect ICI suppression, but also exhibit a remarkable robustness against the NBI. In particular, note that, except for very high values of the SNR, the “WL-ZF-MMOE (RMIC)” equalizer outperforms the “WL-ZF-MMOE (IDFT)” one.

5.1.2. ABER versus SIR

In this experiment, we evaluated the performances of the considered equalizers as a function of the SIR ranging from 0 to 30 dB. With reference to a CP-based system, results of Figure 4 further corroborate the good NBI suppression capabilities of the “WL-ZF-MMOE (RMIC)” equalizer, which largely outperforms the “L-ZF (IDFT),” “L-ZF (RMIC),” and “WL-ZF-MMOE (IDFT)” equalizers, for all the considered values of the SIR. On the other hand, it can be seen from Figure 5 that, for a ZP-based system, both WL equalizers allow one to achieve a significant performance gain with respect to their linear counterparts, by working well even in the presence of strong NBI signal. Specifically, with respect to the “WL-ZF-MMOE (IDFT)” receiver, the “WL-ZF-MMOE (RMIC)” equalizer remarkably saves about 14 dB in transmitter power, for a target ABER of $2 \cdot 10^{-4}$. This evidences that adoption of the RMIC precoder is important not only for perfect WL symbol recovery in the absence of disturbance, but also for improved NBI suppression.

5.2. Environment 2: MC system employing $M = 256$ subcarriers with ZP/CP length $L_r = 16$

In this environment, the CP- and ZP-based MC systems employ $M = 256$ subcarriers, with $L_r = 16$. Observe that, in this case, it results that $W_{\text{nbi}} \approx 0.4/M$, that is, the NBI bandwidth is about 40% of the subcarrier spacing. The baseband discrete-time multipath channel $\{h(m)\}_{m=0}^L$ is a random FIR

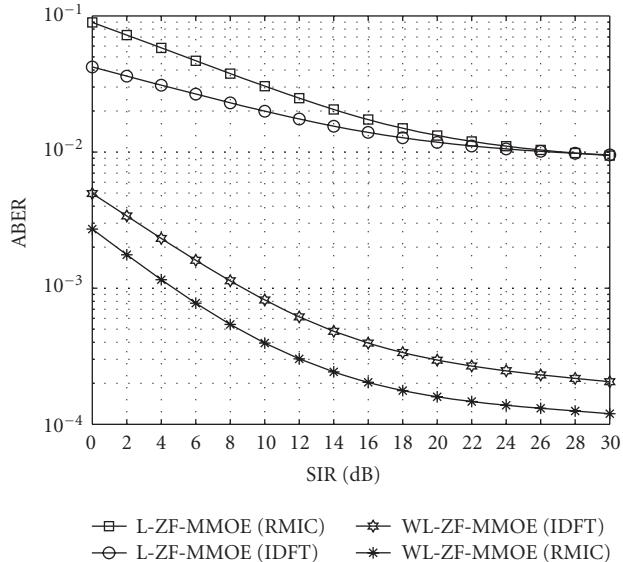


FIGURE 5: ABER versus SIR (Environment 1, ZP-based system, SNR = 20 dB).

filter of order $L = 16$, whose taps are modeled as i.i.d. zero-mean unit-variance complex proper Gaussian random variables, independently varying over 10^3 Monte Carlo runs.

5.2.1. ABER versus SNR

In this experiment, we evaluated the performances of the equalizers compared in the Environment 1, as a function of the SNR ranging from 0 to 30 dB. Figure 6 reports the results for a CP-based, whereas Figure 7 refers to a ZP-based system. Basically, Figures 6 and 7 show the same performance trends of Figures 2 and 3, by further corroborating the effectiveness of the proposed RMIC precoding strategy. It is interesting to observe that, in general, the full-column rank property of the channel matrix \mathcal{H} does not necessarily mean that the inversion of the matrix $\mathcal{H}^H \mathcal{H}$, which is needed to calculate \mathcal{H}^\dagger in (6), is nicely conditioned. In particular, it might happen that, for a large number of subcarriers, the condition number of $\mathcal{H}^H \mathcal{H}$ may be too large and, consequently, the ZF constraint $\mathcal{G}\mathcal{H} = \mathbf{I}_M$ might not be satisfied exactly.⁸ Interestingly, results of Figures 6 and 7 show that this problem does not occur for the RMIC precoder, which not only guarantees that \mathcal{H} is full-column rank for any FIR channel of order $L \leq L_r$, but additionally assures that channel inversion is well-conditioned even when a large number of subcarriers is used.

6. CONCLUSIONS

We considered the problem of deriving mathematical conditions guaranteeing WL-FIR perfect symbol recovery in

⁸ If $\mathcal{H}^H \mathcal{H}$ is near to be singular, matrix \mathcal{H}^\dagger is the minimal norm least-square solution of the ZF constraint $\mathcal{G}\mathcal{H} = \mathbf{I}_M$.

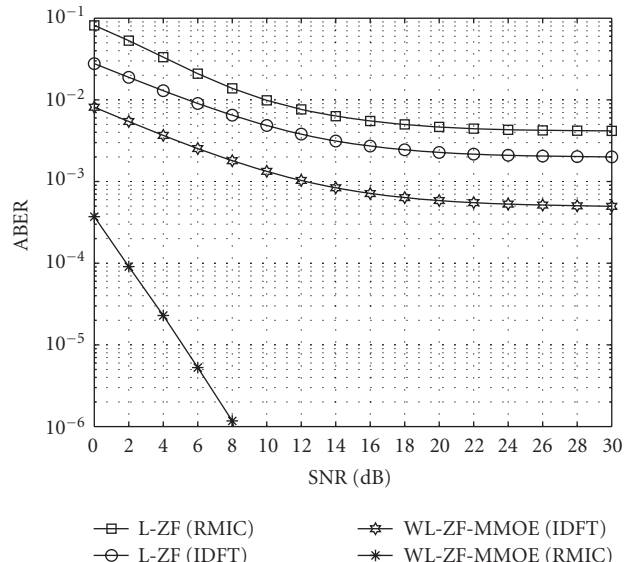


FIGURE 6: ABER versus SNR (Environment 2, CP-based system, SIR = 10 dB).

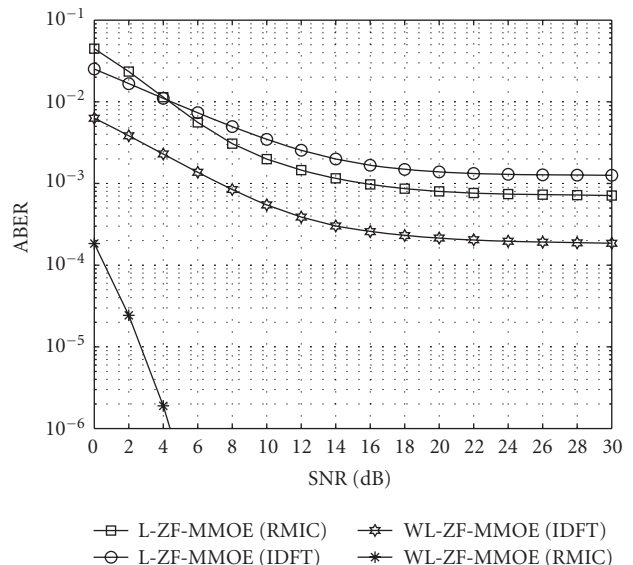


FIGURE 7: ABER versus SNR (Environment 2, ZP-based system, SIR = 10 dB).

the absence of noise for either CP-based or ZP-based MC systems. The conditions derived herein are channel-independent and are expressed in terms of relatively simple design constraints on the linear precoder. Specifically, we have shown that, for both CP- and ZP-based systems, FIR WL-ZF equalization can be guaranteed even when the channel transfer function exhibits nulls on some subcarriers. Moreover, the NBI rejection capabilities of the WL-ZF-MMOE equalizer have been analyzed in the high SNR region, by providing conditions that assure perfect NBI suppression. Finally, in this paper, the proposed universal precoders were not optimized and the channel impulse response was as-

sumed to be exactly known at the receiving side; the interesting extensions of jointly optimal transceiver optimization and blind subspace-based channel estimation are the topic of our current research and will be addressed in a forthcoming paper.

APPENDICES

A. PROOF OF THEOREM 1

Let us consider the case where the channel transfer function $H(z)$ has $0 \leq M_z \leq L$ distinct zeros on the subcarriers $z_{m_1} = e^{i(2\pi/M)m_1}, z_{m_2} = e^{i(2\pi/M)m_2}, \dots, z_{m_{M_z}} = e^{i(2\pi/M)m_{M_z}}$, with $m_1 \neq m_2 \neq \dots \neq m_{M_z} \in \{0, 1, \dots, M-1\}$. In this case, one has $\alpha_{\text{cp}}(m_1) = \alpha_{\text{cp}}(m_2) = \dots = \alpha_{\text{cp}}(m_{M_z}) = 0$ and, thus, the diagonal matrix \mathcal{A}_{cp} is singular with $\text{rank}(\mathcal{A}_{\text{cp}}) = 2(M - M_z)$. Since \mathbf{B}_{cp} and \mathbf{J} are nonsingular, the matrix \mathcal{B}_{cp} is full-column rank by construction. Thus, the matrix $\mathcal{A}_{\text{cp}}\mathcal{B}_{\text{cp}}$ is full-column rank if and only if [31] $\mathcal{N}(\mathcal{A}_{\text{cp}}) \cap \mathcal{R}(\mathcal{B}_{\text{cp}}) = \{\mathbf{0}_{2M}\}$. The null space of \mathcal{A}_{cp} can be readily characterized: an arbitrary vector $\boldsymbol{\mu} = [\boldsymbol{\mu}_1^T, \boldsymbol{\mu}_2^T]^T \in \mathbb{C}^{2M}$, with $\boldsymbol{\mu}_1, \boldsymbol{\mu}_2 \in \mathbb{C}^M$, belongs to $\mathcal{N}(\mathcal{A}_{\text{cp}})$ if and only if $\boldsymbol{\mu}_1 \in \mathcal{N}(\mathbf{A}_{\text{cp}})$ and $\boldsymbol{\mu}_2^* \in \mathcal{N}(\mathbf{A}_{\text{cp}})$. It is easily seen that $\boldsymbol{\mu}_1 \in \mathcal{N}(\mathbf{A}_{\text{cp}})$ if and only if there exists a vector $\boldsymbol{\beta}_1 \in \mathbb{C}^{M_z}$ such that $\boldsymbol{\mu}_1 = \mathbf{S}_z \boldsymbol{\beta}_1$. In the same manner, it can be proven that $\boldsymbol{\mu}_2^* \in \mathcal{N}(\mathbf{A}_{\text{cp}})$ if and only if there exists a vector $\boldsymbol{\beta}_2 \in \mathbb{C}^{M_z}$ such that $\boldsymbol{\mu}_2 = \mathbf{S}_z \boldsymbol{\beta}_2$. Consequently, we can infer that $\boldsymbol{\mu} \in \mathcal{N}(\mathcal{A}_{\text{cp}})$ if and only if there exists a vector $\boldsymbol{\beta} = [\boldsymbol{\beta}_1^T, \boldsymbol{\beta}_2^T]^T \in \mathbb{C}^{2M_z}$ such that $\boldsymbol{\mu} = \boldsymbol{\mathcal{S}}_z \boldsymbol{\beta}$. Hence, an arbitrary vector $\boldsymbol{\mu} \in \mathcal{N}(\mathcal{A}_{\text{cp}})$ also belongs to the subspace $\mathcal{R}(\mathcal{B}_{\text{cp}})$ if and only if there exists a vector $\boldsymbol{\alpha} \in \mathbb{C}^M$ such that $\boldsymbol{\mathcal{S}}_z \boldsymbol{\beta} = \mathcal{B}_{\text{cp}} \boldsymbol{\alpha}$. As a consequence, condition $\mathcal{N}(\mathcal{A}_{\text{cp}}) \cap \mathcal{R}(\mathcal{B}_{\text{cp}}) = \{\mathbf{0}_{2M}\}$ holds if and only if the system of equations $\mathcal{B}_{\text{cp}} \boldsymbol{\alpha} - \boldsymbol{\mathcal{S}}_z \boldsymbol{\beta} = \mathbf{0}_{2M}$ admits the unique solution $\boldsymbol{\alpha} = \mathbf{0}_M$ and $\boldsymbol{\beta} = \mathbf{0}_{2M_z}$. It can be seen [32] that this happens if and only if and only if the matrix $[\mathcal{B}_{\text{cp}}, \boldsymbol{\mathcal{S}}_z] \in \mathbb{C}^{2M \times (M+2M_z)}$ turns out to be full-column rank. Furthermore, since it results [40] that $\text{rank}([\mathcal{B}_{\text{cp}}, \boldsymbol{\mathcal{S}}_z]) = \text{rank}(\boldsymbol{\mathcal{S}}_z) + \text{rank}[(\mathbf{I}_{2M} - \boldsymbol{\mathcal{S}}_z \boldsymbol{\mathcal{S}}_z^*) \mathcal{B}_{\text{cp}}]$, with $\text{rank}(\boldsymbol{\mathcal{S}}_z) = 2M_z$ and $\boldsymbol{\mathcal{S}}_z^* = \boldsymbol{\mathcal{S}}_z^T$ [31], it follows that $\text{rank}([\mathcal{B}_{\text{cp}}, \boldsymbol{\mathcal{S}}_z]) = M + 2M_z$ holds if and only if $\text{rank}[(\mathbf{I}_{2M} - \boldsymbol{\mathcal{S}}_z \boldsymbol{\mathcal{S}}_z^*) \mathcal{B}_{\text{cp}}] = M$.

B. PROOF OF THEOREM 2

When $\sigma_v^2 \rightarrow 0$, evaluation of $\mathcal{P}_{\text{d,min}}$ is complicated by the fact that \mathbf{R}_{dd} becomes singular and, thus, the inverse $(\mathbf{I} \mathbf{R}_{\text{dd}} \mathbf{I}^H)^{-1}$ does not exist. Accounting for (24) and resorting to the limit formula for the Moore-Penrose inverse [38], one has

$$\begin{aligned} \lim_{\sigma_v^2 \rightarrow 0} \mathcal{P}_{\text{d,min}} &= \text{trace} \left[\boldsymbol{\mathcal{G}}_{\text{zf}}^{(f)} \mathcal{L} \mathcal{L}^H (\boldsymbol{\mathcal{G}}_{\text{zf}}^{(f)})^H \right] \\ &\quad - \text{trace} \left[\boldsymbol{\mathcal{G}}_{\text{zf}}^{(f)} \mathcal{L} (\mathbf{\Pi} \mathcal{L})^\dagger \mathbf{\Pi} \mathcal{L} \mathcal{L}^H (\boldsymbol{\mathcal{G}}_{\text{zf}}^{(f)})^H \right] \\ &= \text{trace} \left\{ \boldsymbol{\mathcal{G}}_{\text{zf}}^{(f)} \mathcal{L} \left[\mathbf{I}_{2R_{\text{nb}}} - (\mathbf{\Pi} \mathcal{L})^\dagger (\mathbf{\Pi} \mathcal{L}) \right] \mathcal{L}^H (\boldsymbol{\mathcal{G}}_{\text{zf}}^{(f)})^H \right\} \\ &\quad \mathbf{P}_{\mathcal{N}(\mathbf{\Pi} \mathcal{L})} \in \mathbb{C}^{2R_{\text{nb}} \times 2R_{\text{nb}}} \\ &= \text{trace} \left\{ \boldsymbol{\mathcal{G}}_{\text{zf}}^{(f)} \mathcal{L} \mathbf{P}_{\mathcal{N}(\mathbf{\Pi} \mathcal{L})} \mathcal{L}^H (\boldsymbol{\mathcal{G}}_{\text{zf}}^{(f)})^H \right\}. \end{aligned} \tag{B.1}$$

Observe that the matrix $\mathbf{P}_{\mathcal{N}(\mathbf{\Pi} \mathcal{L})}$ defined in (B.1) represents the orthogonal projector on the subspace $\mathcal{N}(\mathbf{\Pi} \mathcal{L})$. Under condition (C3), the matrix $\mathbf{\Pi} \mathcal{L} \in \mathbb{C}^{(2Q-M) \times 2R_{\text{nb}}}$ turns out to be tall and, thus, the dimension of its null space is equal to the number $2R_{\text{nb}}$ of columns minus $\text{rank}(\mathbf{\Pi} \mathcal{L})$. Due to the fact that $\mathbf{\Pi} \mathcal{H} = \mathbf{O}_{(2Q-M) \times M}$, the columns of \mathcal{H} belong to $\mathcal{N}(\mathbf{\Pi})$, that is, $\mathcal{R}(\mathcal{H}) \subseteq \mathcal{N}(\mathbf{\Pi})$; however, if condition (C4) holds, the subspace $\mathcal{R}(\mathcal{H})$ has the same dimension M of $\mathcal{N}(\mathbf{\Pi})$, thus obtaining $\mathcal{R}(\mathcal{H}) = \mathcal{N}(\mathbf{\Pi})$ which, together with condition (C5), implies that $\mathcal{N}(\mathbf{\Pi}) \cap \mathcal{R}(\mathcal{L}) = \{\mathbf{0}_{2Q}\}$. This last relation is equivalent [38] to $\text{rank}(\mathbf{\Pi} \mathcal{L}) = 2R_{\text{nb}}$, which means that the dimension of $\mathcal{N}(\mathbf{\Pi} \mathcal{L})$ is zero, implying thus $\mathbf{P}_{\mathcal{N}(\mathbf{\Pi} \mathcal{L})} = \mathbf{O}_{2R_{\text{nb}} \times 2R_{\text{nb}}}$, hence $\lim_{\sigma_v^2 \rightarrow 0} \mathcal{P}_{\text{d,min}} = 0$.

ACKNOWLEDGMENT

This work is partially supported by Italian National project Wireless 8O2.16 Multi-antenna mEsh Networks (WOMEN) under Grant no. 2005093248.

REFERENCES

- [1] Z. Wang and G. B. Giannakis, "Wireless multicarrier communications: where Fourier meets Shannon," *IEEE Signal Processing Magazine*, vol. 17, no. 3, pp. 29–48, 2000.
- [2] T. Starr, J. M. Cioffi, and P. J. Silvermann, *Understanding Digital Subscriber Line Technology*, Prentice-Hall, Englewood Cliffs, NJ, USA, 1999.
- [3] "HomePlug 1.0 specification," <http://www.homeplug.org/>.
- [4] "IEEE 802.11 working group for wireless local area networks," <http://grouper.ieee.org/groups/802/11/>.
- [5] ETSI Normalization Committee, "High performance radio local area networks (HIPERLAN) type 2," <http://www.etsi.org/>.
- [6] ETSI Normalization Committee, "Radio broadcasting systems, digital audio broadcasting (DAB) to mobile, portable, and fixed receivers," <http://www.etsi.org/>.
- [7] ETSI Normalization Committee, "Digital video broadcasting (DVB): framing structure, channel coding and modulation for digital terrestrial television," <http://www.etsi.org/>.
- [8] A. Scaglione, G. B. Giannakis, and S. Barbarossa, "Redundant filterbank precoders and equalizers. I. Unification and optimal designs," *IEEE Transactions on Signal Processing*, vol. 47, no. 7, pp. 1988–2006, 1999.
- [9] A. Scaglione, G. B. Giannakis, and S. Barbarossa, "Redundant filterbank precoders and equalizers. II. Blind channel estimation, synchronization, and direct equalization," *IEEE Transactions on Signal Processing*, vol. 47, no. 7, pp. 2007–2022, 1999.
- [10] B. Muquet, Z. Wang, G. B. Giannakis, M. de Courville, and P. Duhamel, "Cyclic prefixing or zero padding for wireless multicarrier transmissions?" *IEEE Transactions on Communications*, vol. 50, no. 12, pp. 2136–2148, 2002.
- [11] A. Scaglione, S. Barbarossa, and G. B. Giannakis, "Filterbank transceivers optimizing information rate in block transmissions over dispersive channels," *IEEE Transactions on Information Theory*, vol. 45, no. 3, pp. 1019–1032, 1999.
- [12] D. Darsena, G. Gelli, L. Paura, and F. Verde, "Widely linear equalization and blind channel identification for interference-contaminated multicarrier systems," *IEEE Transactions on Signal Processing*, vol. 53, no. 3, pp. 1163–1177, 2005.
- [13] D. Darsena, G. Gelli, L. Paura, and F. Verde, "A constrained maximum-SINR NBI-resistant receiver for OFDM systems,"

- IEEE Transactions on Signal Processing*, vol. 55, no. 6, pp. 3032–3047, 2007.
- [14] D. Darsena, G. Gelli, L. Paura, and F. Verde, “Joint equalisation and interference suppression in OFDM systems,” *Electronics Letters*, vol. 39, no. 11, pp. 873–874, 2003.
- [15] D. Darsena, G. Gelli, L. Paura, and F. Verde, “NBI-resistant zero-forcing equalizers for OFDM systems,” *IEEE Communications Letters*, vol. 9, no. 8, pp. 744–746, 2005.
- [16] P. J. Schreier and L. L. Scharf, “Second-order analysis of improper complex random vectors and processes,” *IEEE Transactions on Signal Processing*, vol. 51, no. 3, pp. 714–725, 2003.
- [17] J. Eriksson and V. Koivunen, “Complex random vectors and ICA models: identifiability, uniqueness, and separability,” *IEEE Transactions on Information Theory*, vol. 52, no. 3, pp. 1017–1029, 2006.
- [18] B. Picinbono and P. Chevalier, “Widely linear estimation with complex data,” *IEEE Transactions on Signal Processing*, vol. 43, no. 8, pp. 2030–2033, 1995.
- [19] H. L. Van Trees, *Optimum Array Processing*, John Wiley & Sons, New York, NY, USA, 2002.
- [20] G. Gelli, L. Paura, and F. Verde, “On the existence of FIR zero-forcing equalizers for nonredundantly precoded transmissions through FIR channels,” *IEEE Signal Processing Letters*, vol. 12, no. 3, pp. 202–205, 2005.
- [21] Z. Ding and G. Li, “Single-channel blind equalization for GSM cellular systems,” *IEEE Journal on Selected Areas in Communications*, vol. 16, no. 8, pp. 1493–1505, 1998.
- [22] D. Darsena, G. Gelli, L. Paura, and F. Verde, “Subspace-based blind channel identification of SISO-FIR systems with improper random inputs,” *Signal Processing*, vol. 84, no. 11, pp. 2021–2039, 2004, special issue on Signal Processing in Communications.
- [23] W. H. Gerstacker, R. Schober, and A. Lampe, “Receivers with widely linear processing for frequency-selective channels,” *IEEE Transactions on Communications*, vol. 51, no. 9, pp. 1512–1523, 2003.
- [24] S. Benedetto and E. Biglieri, *Principles of Digital Communications with Wireless Applications*, Kluwer Academic/Plenum, New York, NY, USA, 1999.
- [25] International Telecommunication Union (ITU) and Radio-communication Study Groups, “Study of the required geographic coordination distance between a HAPS TDMA system and adjacent system IMT-2000 terrestrial mobile stations operating in the same frequency band,” document 8-1/368-E, May 1988.
- [26] J. A. C. Bingham, *The Theory and Practice of Modem Design*, John Wiley & Sons, New York, NY, USA, 1988.
- [27] P. Siohan, C. Siclet, and N. Lacaille, “Analysis and design of OFDM/OQAM systems based on filterbank theory,” *IEEE Transactions on Signal Processing*, vol. 50, no. 5, pp. 1170–1183, 2002.
- [28] G. Gelli and F. Verde, “Blind subspace-based channel identification for quasi-synchronous MC-CDMA systems employing improper data symbols,” in *Proceedings of the 14th European Signal Processing Conference (EUSIPCO '06)*, Florence, Italy, September 2006.
- [29] P. Ciblat and E. Serpedin, “A fine blind frequency offset estimator for OFDM/OQAM systems,” *IEEE Transactions on Signal Processing*, vol. 52, no. 1, pp. 291–296, 2004.
- [30] T. Fusco and M. Tanda, “Blind frequency-offset estimation for OFDM/OQAM systems,” *IEEE Transactions on Signal Processing*, vol. 55, no. 5, pp. 1828–1838, 2007.
- [31] R. Penrose, “A generalized inverse for matrices,” *Proceedings of the Cambridge Philosophical Society*, vol. 51, pp. 406–413, 1955.
- [32] R. A. Horn and C. R. Johnson, *Matrix Analysis*, Cambridge University Press, New York, NY, USA, 1990.
- [33] F. D. Neeser and J. L. Massey, “Proper complex random processes with applications to information theory,” *IEEE Transactions on Information Theory*, vol. 39, no. 4, pp. 1293–1302, 1993.
- [34] S. V. Schell, “A separability theorem for $2M$ conjugate-symmetric signals impinging on an M sensor array,” *IEEE Transactions on Signal Processing*, vol. 45, no. 3, pp. 789–792, 1997.
- [35] A. Chevreuil and P. Loubaton, “Blind second-order identification of FIR channels: forced cyclostationarity and structured subspace method,” *IEEE Signal Processing Letters*, vol. 4, no. 7, pp. 204–206, 1997.
- [36] E. Serpedin and G. B. Giannakis, “Blind channel identification and equalization with modulation-induced cyclostationarity,” *IEEE Transactions on Signal Processing*, vol. 46, no. 7, pp. 1930–1944, 1998.
- [37] D. Slepian, “Prolate spheroidal wave functions, Fourier analysis, and uncertainty. V. The discrete case,” *Bell System Technical Journal*, vol. 57, no. 5, pp. 1371–1430, 1978.
- [38] A. Ben-Israel and T. N. E. Greville, *Generalized Inverses*, Springer, Berlin, Germany, 2002.
- [39] R. T. Behrens and L. L. Scharf, “Signal processing applications of oblique projection operators,” *IEEE Transactions on Signal Processing*, vol. 42, no. 6, pp. 1413–1424, 1994.
- [40] G. Marsaglia and G. P. H. Styan, “Equalities and inequalities for ranks of matrices,” *Linear and Multilinear Algebra*, vol. 2, no. 3, pp. 269–292, 1974.

Composition Comments

1. Should we change "L (normal text)" to " L (normal math)"? Please check.
2. We changed "issues" into the highlighted "issue." Please check.
3. We changed "Lemma 2" to the highlighted "Theorem 2." Please check.